13th International Conference on Defects–Recognition, Imaging and Physics in Semiconductors

DRIP XIII

FINAL PROGRAM

September 13-17, 2009
Oglebay Resort & Conference Center
Wheeling, West Virginia USA

Sponsored by:

TMS

www.tms.org/meetings/specialty/drip09/home.html

Welcome to the DRIP XIII Conference

TMS is proud to sponsor the 13th International Conference on Defects — Recognition, Imaging, and Physics in Semiconductors!

As semiconductor technology has matured, so have the techniques for detection, identification and imaging of defects. Decreasing feature size, increasing wafer size and purity level, reduction of layer thickness and introduction of new materials have presented new challenges at every stage of semiconductor technology development. This evolution of the field continues today. These new challenges will be the focus of DRIP XIII.

ORGANIZING COMMITTEE

Mark Dexter, *Texas Instruments, USA*
Michael Dudley, *SUNY Stony Brook, USA*
Piotr Edelman, *SDI, USA*
Mark S. Goorsky, *UCLA, USA*
Andrew M. Hoff, *University of South Florida, USA*
Philip G. Neudeck, *NASA GRC, USA*
Steven A. Ringel, *The Ohio State University, USA*
Marek Skowronski, *Carnegie Mellon University, USA*
Peilin Song, *IBM T.J. Watson Research Center, USA*
Robert E. Stahlbush, *Naval Research Laboratory, USA*
Michio Tajima, *Japan Space Exploration Agency, Japan*
Jens W. Tomm, *Max Born Institute, Germany*

INTERNATIONAL STEERING COMMITTEE

Jean-Pierre Fillard, *Honorary Member, France*
Tomoya Ogawa, *Honorary Member, Japan*
Martina Baeumler, *Germany*
Anna Cavallini, *Italy*
Piotr Edelman, *USA*
Cesare Frigeri, *Italy*
Juan Jimenez, *Spain*
Jean-Pierre Landesman, *France*
Alan Mickelson, *USA*
Paul Montgomery, *France*
Takashi Sekiguchi, *Japan*
Marek Skowronski, *USA*
Michio Tajima, *Japan*
Jens W. Tomm, *Germany*
Zhanguo Wang, *China*
Jan Weyher, *Poland, The Netherlands*
Deren Yang, *China*

Table of Contents

CONFERENCE REGISTRATION

Conference Registration Area
Sunday, September 13..... 4 to 9 p.m.
Monday, September 14..... 7:30 a.m. to 4 p.m.
Tuesday, September 15 ..... 8 a.m. to 1 p.m.
Wednesday, September 16..... 8 a.m. to 4 p.m.
Thursday, September 17 ..... 8 a.m. to noon

TECHNICAL SESSIONS

Glessner Auditorium
Monday, September 14 and Wednesday, September 16 ..... 8:30 a.m. to 3:30 p.m.
Tuesday, September 15 and Thursday, September 17 ..... 8:30 a.m. to 12:30 p.m.

CLOSING REMARKS

Thursday, September 17 ..... 12:30 to 12:45 p.m.

INVITED SPEAKERS

Xianrong Huang
State University of New York at Stony Brook, *USA*
"Developing bright field synchrotron imaging techniques with ultrahigh spatial and strain sensitivity"

Maria Kaniewska
Institute of Electron Technology, *Poland*
"Classification of energy levels in quantum dot structures by means of depleted layer spectroscopy methods"

Christian Kisielowski
Lawrence Berkeley National Laboratory, *USA*
"The next generation electron microscopes: Opportunities and challenges beyond the current state of the art"

Bernd Sumpf
Ferdinand Braun Institute, *Germany*
"Reliability investigations on high-power, high-brightness semiconductor lasers"

Hidekazu Tsuchida
Central Research Institute Electric Power Industry, *Japan*
"Analysis of defect formation in 4H-SiC epitaxial growth by X-ray topography"

NETWORKING & SOCIAL EVENTS

WELCOME RECEPTION

Sunday.....7:30 to 9 p.m.
Banquet Rooms 1-3 (second floor)
Enjoy hors d'oeuvres and cocktails while mingling with fellow attendees

COFFEE BREAKS

Glessner Auditorium
Monday through Thursday.....10 to 10:30 a.m.

POSTER VIEWING/RECEPTION

Banquet Rooms 1-3
Monday.....4:30 to 7 p.m.

AFTERNOON BREAKS

Glessner Auditorium
Monday.....3:30 to 4 p.m.
Wednesday.....3:30 to 4 p.m.

LUNCH

Banquet Rooms 1-3
Monday through Wednesday.....12:30 to 1:30 p.m.

CONFERENCE BANQUET

Tuesday
Terrace Room
Reception.....6 to 6:45 p.m.
Banquet Rooms 1-3
Banquet.....6:45 to 8:30 p.m.

LOCAL ATTRACTIONS

Oglebay Resort Activities

Outdoor Activities

Nestled amidst the beauty of West Virginia's mountains, Oglebay offers 1700 acres of relaxation and recreation. Choose from dozens of activities to please a variety of discriminating tastes - from the state's only accredited zoo, to outdoor adventures including golf, tennis, and horseback riding.

Many of the recreational amenities at Oglebay are offered year round, weather permitting - including golf on the Crispin Course. Affordably priced packages that include many of Oglebay's activities are offered throughout the year. Those interested in spending the entire day participating in multiple activities may want to purchase an activity band at the resort's front desk, which allows access to many of the fun things Oglebay has to offer.

Indoor Activities

At Wilson Lodge, you will be treated to the very best. After your workout in the complete fitness center, relax in the heated indoor pool, Jacuzzi or sauna. The West Spa at Oglebay offers relaxing and therapeutic services, utilizing the finest products and equipment.

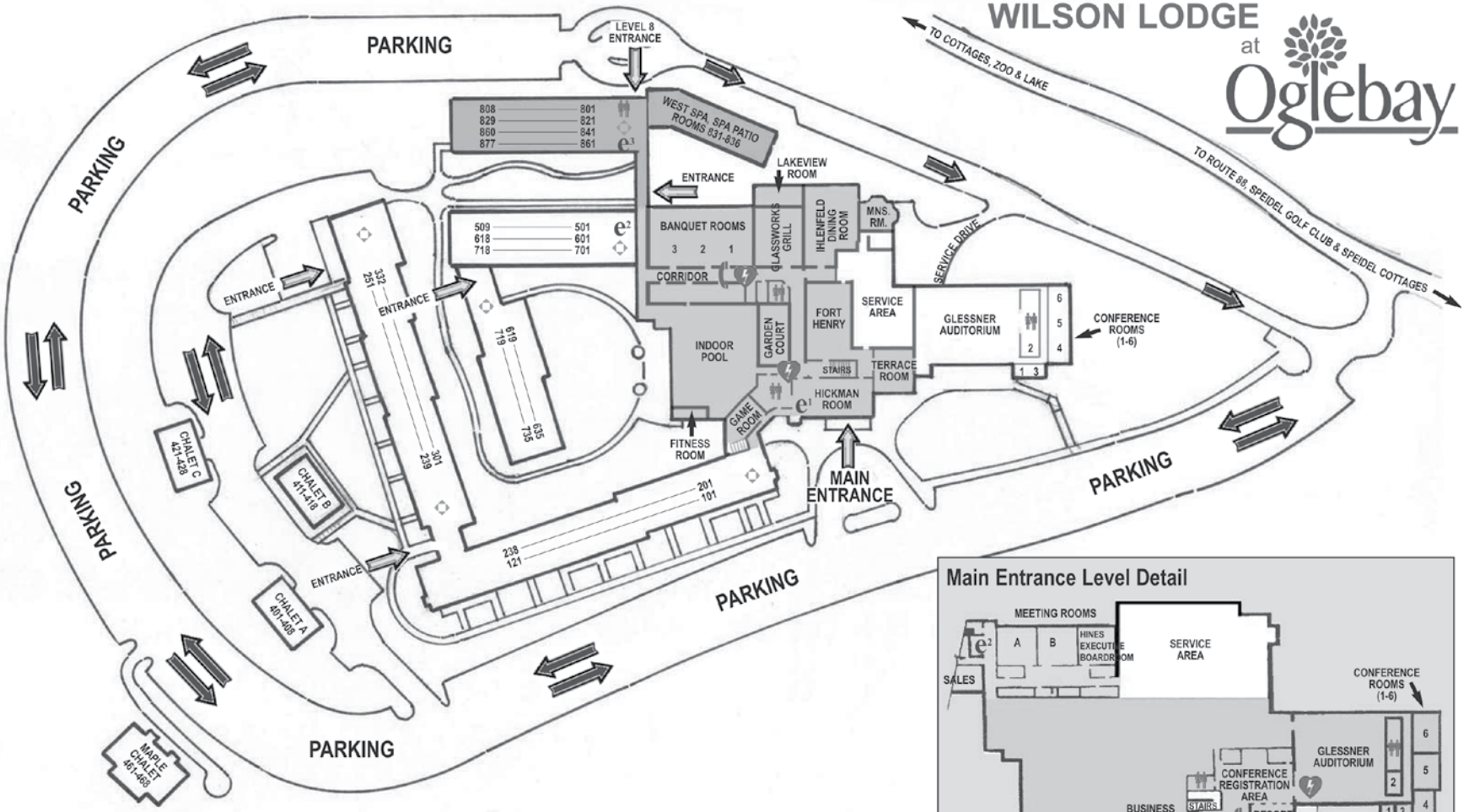

Lobby / Main Entrance Level	Front Desk, Resort Shop, Information Desk, Business Center, Glessner Auditorium, Lobby Conference Rooms 1-6
Level 5	Take Main Stairs from Lobby or use Elevator 1 (e¹) to 2nd Floor (Level 6) then take Elevator 2 (e²) to: Meeting Rooms A, B, Hines Executive Board Room, Sales Office, Spa Patio
2nd Floor/ Level 6	Take Main Stairs from Lobby or use Elevator 1 (e¹) to 2nd Floor (Level 6) to: Banquet Rooms 1, 2 & 3, Fort Henry Room, Terrace Room, Hickman Lounge, Ihlenfeld Dining Room, GlassWorks Grill, Pool & Fitness Center, Walkway to 800 Level and Spa
Level 8/ West Spa	Take Main Stairs from Lobby or use Elevator 1 (e¹) to 2nd Floor (Level 6), then proceed past Banquet Rooms and turn right to the 800 level walkway to Elevator 3 (e³). Spa entrance is on Level 3. Spa Patio entrance is on Level 5

- e Elevators
- Restrooms
- Ice & Vending
- Telephone
- Building Entrance
- Automated External Defibrillator


Oglebay
To Wheeling
88
Gardens
Mansion Museum
Garden Center Amphitheater
Gourmet Shop Visitors Center
Glass Shop & Museum
MAP LEGEND
Information
Snack Bar
Restrooms
Reserved Picnic Sites
Dining/ Restaurant
Recycling Drop-off Container
Picnic Overlook
Sites 2-6
Good Zoo
Nature Express Shop
Benedum Planetarium
Schenk Lake
Cascading Waters
Pedal Boats
Fishing
Wilson Lodge
Resort Shop
Restaurants
Lodge/Cottage Check-in
Playground
Wagon Shed
Hess Shelter
Mini Golf
Levenson Shelter/ Site One
Camp Russel
Environmental Center
Observatory
Sites15-20
OPCA Shelter
Cottage Site C
Cottage Site A
Cottage Site B
RH
LI
HE
M
HO
CB
GI
FO
DA
MA
AR
AS
BE
CH
DO
EL
WA
C
G
K
L
A
B
D
E
F
U
V
W
O
Y
Z
T
S
R
Q
I
J
H
N
W
E
S
To Wheeling
Falls Entrance
Waddles Run Road

FACILITY MAP

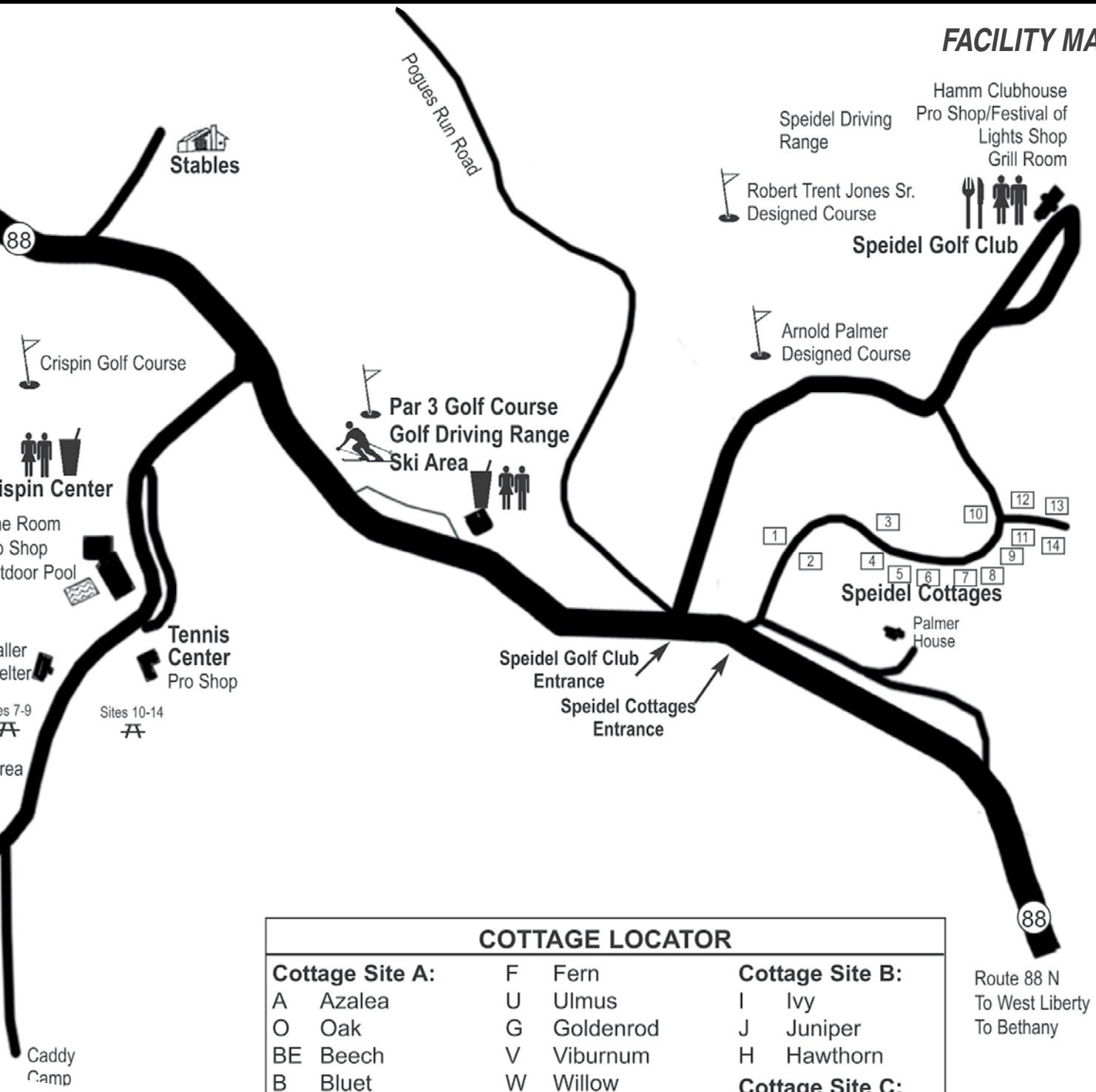

COTTAGE LOCATOR

Cottage Site A:

A	Azalea
O	Oak
BE	Beech
B	Bluet
Q	Quince
CH	Chestnut
C	Clover
R	Redbud
D	Daisy
S	Sumac
DO	Dogwood
E	Edelweiss
T	Tulip
EL	Elderberry
F	Fern
U	Ulmus
G	Goldenrod
V	Viburnum
W	Willow
Y	Yucca
Z	Zelkova
K	Kalmia
WA	Waddington
L	Laurel
AS	Ash

Cottage Site B:

I	Ivy
J	Juniper
H	Hawthorn

Cottage Site C:

AR	Aster
DA	Daffodil
GI	Ginkgo
FO	Forsythia
HO	Holly
LI	Lilac
RH	Rhododendron
MA	May
CB	Chambers
HE	Hess

COMPUTER/NETWORK FACILITIES

Internet Access
Complimentary WiFi access is available for DRIP XIII attendees in Banquet Rooms 1-3 and the Glessner Auditorium. In addition, the Hickman Room in the Wilson Lodge is WiFi accessible.

Messages
A message board will be located near the DRIP registration desk for attendee use.

Americans with Disabilities Act
TMS strongly supports the federal Americans with Disabilities Act (ADA) which prohibits discrimination against, and promotes public accessibility for those with disabilities. In support of and compliance with this Act, we ask that those attendees requiring specific equipment or services indicate their needs on the enclosed housing form or by contacting the TMS Meeting Services Department.

Audio/Video Recording Policy
TMS reserves the rights to any audio and video reproduction of all presentations at every TMS sponsored meeting. Recording of sessions (audio, video, still photography, etc.) intended for personal use, distribution, publication, or copyright without the express written consent of TMS and the individual authors is strictly prohibited.

Dress
Casual clothing is in order with a sweater or light jacket occasionally needed for the evenings. Layered clothing is recommended for cooler days or in air-conditioned buildings. The average afternoon temperature in the middle of September reaches highs in the upper 70 degrees and the nighttime temperature drops to between 55 and 65 degrees.

TRAVEL INFORMATION

Airport Shuttle
Complimentary shuttle will depart Oglebay Resort for the Pittsburgh International Airport on Thursday, September 17, 2009, at 1 and 3 p.m. Please notify the DRIP XIII Conference registration desk if you have a change to your departure time.

Limousine Service
24-hour transportation service between Pittsburgh International Airport and Oglebay Resort is provided by Airport Limousine. Attendees should secure reservations either by phone at (304) 232-1175 for a cost of $74 for one-way service, or via the Internet at: **http://www.wheelinglimo.com/** for a one-way fee of $70. To make an Internet reservation, please click on the Oglebay Shuttle Request Form and select **DRIP 2009** on the School/Institute list.

BE MATERIALS-MINDED

TMS is committed to environmental responsibility as we fulfill our mission to promote global science and engineering by going green at our headquarters, conferences and through membership communication.

Please join us in our effort by using the recycling bins that will be available for unwanted programs and badge holders in the registration area.

Be materials-minded. *Join* TMS *in reducing, reusing and recycling.*

JOURNAL OF ELECTRONIC MATERIALS

Proceedings will appear as a special issue of the *Journal of Electronic Materials (JEM)*. *JEM* is a monthly archival technical journal published by TMS and the Institute of Electrical and Electronics Engineers (IEEE). The journal contains technical papers detailing critical new developments in the electronic materials field, as well as invited and contributed review papers on topics of current interest. Visit the *JEM* home page for more information.

FOR MORE INFORMATION . . .

For inquiries regarding proceedings, please contact the Proceedings Editors:

Dr. P. Edelman, SDI
Tampa, FL
Phone: (813) 977-2244
E-mail: piotr@sditampa.com

Prof. Andrew M. Hoff, University of South Florida
Tampa, FL
Phone: (813) 974-4958
E-mail: hoff@eng.usf.edu

Become a TMS member today and pay only $115 for the remainder of 2009 through 2010!

As your professional partner for career advancement, TMS offers you technical information and networking opportunities specific to your field. Enjoy these benefits:

- A print and electronic subscription to *JOM*, the magazine that explores the traditional, innovative, and revolutionary issues in the minerals, metals, and materials fields.
- A members-only discount on an individual subscription to *JEM*, a joint TMS and IEEE publication.
- Networking opportunities with a prestigious membership through international conferences.
- Discount on TMS publications and conference fees.
- Access to the TMS organizational network through the searchable Online Membership Directory.
- Job and Financial Security Resources Center.
- Plus an array of other membership benefits and services!

To become a member, complete a TMS application and return it to the TMS Registration Desk during the conference, along with your $115 membership fee. You may also join via the TMS web site at **www.tms.org/Society/membership.html**, or mail your application to TMS Headquarters,184 Thorn Hill Road, Warrendale, PA 15086, USA. For more information, visit the TMS web site, contact the TMS Membership Department at membership@tms.org, or call (724) 776-9000, ext 241.

ATTENTION STUDENTS

Become a member of the Material Advantage student program for just $25 and receive the benefits of four varied materials organizations!

ACerS —The American Ceramic Society
AIST—Association for Iron & Steel Technology
ASM—ASM International
TMS—The Minerals, Metals & Materials Society

For full details on benefits, including scholarships and awards totaling more than $600,000, visit **www.materialadvantage.org**. Material Advantage: Everything Else is Immaterial!

MATERIAL™ ADVANTAGE
The Student Program for Materials Science and Engineering
Everything Else Is Immaterial

ABOUT TMS

Headquartered in the United States but international in both its membership and activities, The Minerals, Metals & Materials Society (TMS) is a rare professional organization that encompasses the entire range of materials and engineering, from minerals processing and primary metals production to basic research and the advanced applications of materials.

TMS is a member-driven professional society consisting largely of scientists and engineers working in industry, academia and government, as well as students studying in the materials field. Included among 11,000 professional and student members are metallurgical and materials engineers, scientists, researchers, educators, and administrators from more than 70 countries on six continents.

TMS' mission is to promote the global science and engineering professions concerned with minerals, metals, and materials. To learn more, visit **www.tms.org**

TMS

TMS & SOCIAL NETWORKING

TMS has joined the world of social networking to improve its global presence and further engage members.

Become a Fan of the TMS Page on ***Facebook*** to post your conference experiences, continue your networking connections, or post comments, discussions, conference photos or videos.

Join the TMS ***LinkedIn*** group page to post or start discussions, or share your conference photos or view the TMS photo stream on ***Flickr***.

AT-A-GLANCE

Monday, September 14, 2009

Tuesday, September 15, 2009

Wednesday, September 16, 2009

Thursday, September 17, 2009

Quantum Confined Structures

Monday AM Room: Glessner Auditorium
September 14, 2009 Location: Oglebay Resort & Conference Center

Session Chair: Michael Dudley, Stony Brook University

8:30 AM Introductory Comments

8:35 AM Invited
Classification of Energy Levels in Quantum Dot Structures by Means of Depleted Layer Spectroscopy Methods: *Maria Kaniewska*[1]; Olof Engström[2]; Mariusz Kaczmarczyk[1]; [1]Institute of Electron Technology; [2]Chalmers University of Technology

The coexistence of quantum confined energy levels and defect energy levels in quantum dot (QD) structures may cause difficulties in distinguishing between their different origin when using DLTS. For the functioning of QDs in practical devices, it is important to be able to separate the influence of such energy levels from those of the QDs. Using InAs/GaAs QDs as demonstration vehicles, we present methodologies to obtain such a classification by DLTS. QD-related spectra measured as a function of repetition frequency of electrical pulses, f, or temperature, T, and reverse voltage, V, are depicted as contour plots on (f, V)- and (T, V)-planes, thus reflecting the complex thermal and tunneling emission of electrons from the ground and excited states. Defect-related levels in reference samples without QDs give rise to different contour patterns and undergo modification exhibiting double-peak structured emission when defects are agglomerated in the vicinity of the QD plane.

9:05 AM
Electrical Properties of Si Nanowire Devices Characterized with Scanning Probe Microscopy: *Sung-Soo Bae*[1]; Zhiyong Li[2]; Nathaniel Quitoriano[2]; Theodore Kamins[2]; Regina Ragan[1]; [1]University of California, Irvine; [2]Hewlett-Packard Laboratories

Fundamental studies of how localized charged defects affect current transport along Si nanowires in field effect transistor architecture were performed in order to gain insight into how to fabricate reproducible sensors on this material platform. A change in lateral electron conductivity along nanowires that results due to interactions of (bio)molecules on nanowire surfaces has been attributed to a change in surface charge on nanowires. Yet, it is not clear if sensitivity to biomolecular binding events (and also sensitivity to non-specific events) is enhanced by the presence of defects on the surface. Using scanning Kelvin probe microscopy, we investigated localized changes in electronic structure of Si nanowires and found that localized potential changes were correlated with defects and/or impurities. Nanowires fabricated with top-down and bottom-up methods were compared where the latter demonstrated less variation of surface potential.

9:20 AM
Cross-Sectional Scanning Tunneling Microscopy and Spectroscopy of InAs Quantum Dots in GaAs: Sandeep Gaan[1]; *Randall Feenstra*[1]; John Walker[1]; Elias Towe[1]; [1]Carnegie Mellon University

We have studied InAs/GaAs quantum-dot heterostructures using cross-sectional scanning tunneling microscopy and spectroscopy. Samples were grown by molecular beam epitaxy on n-type GaAs substrates. Individual quantum dots are clearly resolved in the images, and tunneling spectra were acquired at various distances from the dots. We find that spectra acquired 3-4 nm from the dots show a clear peak located in the upper part of the GaAs bandgap, which we associate with the lowest confined state of the InAs conduction band. Spectra acquired directly on the dots display large broadening of this feature, however, apparently due to non-equilibrium occupation of the state by the tunneling electrons. From the spectra we directly estimate a lowest confined state energy of 0.16 ± 0.03 eV below the GaAs conduction band edge.

9:35 AM
Investigation of Optical Properties of InGaN/(AlIn)GaN Multi Quantum Wells for Blue Lasers by Cathodoluminescence: *Ute Zeimer*[1]; Uwe Jahn[2]; Veit Hoffmann[1]; Markus Weyers[1]; Michael Kneissl[3]; [1]Ferdinand-Braun-Institut für Höchstfrequenztechnik; [2]Paul-Drude-Institut für Festkörperelektronik; [3]Technische Universität Berlin, Institut für Festkörperphysik

To expanded the wavelength range of semiconductor lasers based on InGaN/(AlIn)GaN multi quantum wells (MQWs) to 450 nm and beyond the indium concentration in the quantum wells has to be increased. We investigate the influence of both the reduction of growth temperature as well as the increase of the QW thickness on the crystalline quality and defect structure of MQWs grown on sapphire substrate by cathodoluminescence (CL) at 6 K, secondary electron (SE) imaging and atomic force microscopy (AFM). The CL investigations show a local wavelength distribution which is connected to growth spirals. This can be explained by a higher local QW thickness and/or a higher indium concentration in the centre of the spirals. Small randomly distributed surface pits attributed to dislocations show only very weak contrasts in monochromatic CL images. Special emphasis will be devoted to the role of dislocations on the nonradiative recombination processes in InGaN MQWs.

9:50 AM
Effects of Epitaxial Graphene Stacking, Strain, and Thickness Uniformity on Carrier Mobility: *Joshua Robinson*[1]; Joseph Tedesco[2]; Mark Fanton[1]; David Snyder[1]; Glenn Jernigan[2]; Paul Campbell[2]; Rachel Myers-Ward[2]; Charles Eddy[2]; D. Gaskill[2]; [1]Pennsylvania State University EO Center; [2]Naval Research Laboratory

We report results of Raman spectroscopy studies of large-area epitaxial graphene grown on SiC. Our work reveals unexpectedly large variation in Raman shift resulting from graphene strain inhomogeneity, which is shown to be correlated with physical topography by coupling Raman spectroscopy with atomic force microscopy. We show that graphene strain can vary over a distance shorter than 300nm, and may be uniform only over roughly 1 µm. Additionally, we have examined epitaxial graphene with mobility values of 25 – 18,100 cm2/Vs, and show that Raman topography is a vital tool for rapid identification of high mobility material. The Hall mobility of epitaxial graphene on the Si-face of SiC is not only highly dependent on thickness uniformity, but also on mono-layer strain uniformity. High mobility epitaxial graphene grown on the C-face of SiC is dependent on graphene layer stacking.

10:05 AM Break

Electron Beam Imaging

Monday AM Room: Glessner Auditorium
September 14, 2009 Location: Oglebay Resort & Conference Center

Session Chair: Marek Skowronski, Carnegie Mellon University

10:30 AM Invited
The Next Generation Electron Microscopes: Opportunities and Challenges beyond the Current State of the Art: *Christian Kisielowski*[1]; [1]Lawrence Berkeley National Laboratory

This paper addresses advances in electron microscopy that were accomplished over the past years with the incorporation of new electron optical components such as aberration correctors, monochromators or high brightness guns. Many of these developments are currently pursued within the DoE's TEAM project.[1,2] As a result electron microscopy has reached 0.5 Å resolution. In this paper it is shown how the resolution improvement has helped to boost signal to noise ratios enabling a detection of single atoms across the Periodic Table of Elements. The described achievements allow for investigations of single point defects even if generated in two-dimensional sheets of materials such as graphene or single layers of BN. Further it is now possible to access depth information from single projections with a precision that has reached interatomic distances. Beam induced atom motion is found to be a significant source of noise in images of single atoms. [1]http://ncem.lbl.gov/team/TEAMpage/TEAMpage.html [2]C. Kisielowski, B. Freitag, M. Bischoff, H. van Lin, S. Lazar, G. Knippels, P. Tiemeijer, M. van der Stam, S. von Harrach, M. Stekelenburg, M. Haider, H. Muller, P. Hartel, B.

Kabius, D. Miller, I. Petrov, E. Olson, T. Donchev, E.A. Kenik, A. Lupini, J. Bentley, S. Pennycook, A.M. Minor, A.K. Schmid, T. Duden, V. Radmilovic, Q. Ramasse, R. Erni, M. Watanabe, E. Stach, P. Denes, U. Dahmen, /Microscopy and Microanalysis/ *14*, 454-462 (2008).

11:00 AM

Diffraction Contrast of Threading Dislocations in GaN and 4H-SiC Epitaxial Layers Using Electron Channeling Contrast Imaging: *Mark Twigg*[1]; Yoosuf Picard[1]; Joshua Caldwell[1]; Charles Eddy[1]; Michael Mastro[1]; Ronald Holm[1]; Philip Neudeck[2]; Andrew Trunek[3]; J. Powell[4]; [1]Naval Research Laboratory; [2]NASA Glenn Research Center; [3]OAI; [4]Sest, Inc.

Forescattered electron channeling contrast imaging (ECCI) offers the potential of imaging and analyzing extended defects in a scanning electron microscope (SEM). We have recorded and simulated ECCI images of a sample with features that are relatively easily studied and modeled: those based on specially engineered 4H-SiC mesa substrates. These mesas serve as substrates for both homoepitaxial 4H-SiC layers and heteroepitaxial GaN layers in which images of threading dislocations (TDs) have been recorded using ECCI and found to strongly resemble diffraction contrast simulations of TD intensity profiles. Burgers vector identification was confirmed through observations of the rotational direction of atomic step spirals associated with various screw dislocations. For the case of GaN layers, both threading edge dislocations (TEDs) and threading mixed dislocations (TMDs) are identified. It is also seen that TEDs mark low-angle grain boundaries in GaN layers, in accord with plan-view TEM observations.

11:15 AM

Identifying the Influence of Dislocations on 4H-SiC Substrate Step-Morphology and GaN Diode Performance Using Electron Channeling Contrast Imaging: *Yoosuf Picard*[1]; Mark Twigg[1]; Joshua Caldwell[1]; Charles Eddy[1]; Michael Mastro[1]; Ronald Holm[1]; Phillip Neudeck[2]; Andrew Trunek[2]; J. Powell[2]; [1]US Naval Research Laboratory; [2]NASA Glenn Research Center

Electron channeling contrast imaging (ECCI) is a scanning electron microscopy (SEM) technique capable of imaging individual dislocations in crystalline materials. Similar to transmission electron microscopy (TEM), ECCI employs diffraction contrast in order to allow direct dislocation imaging as well as Burgers vector identification. We employ ECCI to image screw dislocations that act as persistent atomic step sources in specially engineered 4H-SiC mesa substrates. Mesa substrates with no surface penetrating screw dislocations are nearly free of atomic steps. ECCI is also used to characterize heteroepitaxial GaN film-based devices deposited on these mesa substrates. The screw and edge dislocation density of individual GaN diodes (p-n junctions) are determined by ECCI and correlated to measured ultraviolet (UV) electroluminescence (EL) output. GaN deposited on nearly step-free 4H-SiC show an order of magnitude reduction in screw dislocation densities, yielding a 20-50% increase in UV-EL output.

11:30 AM

The Origin of Threading Dislocations in GaN Films: *Michelle Moram*[1]; Carsten Ghedia[1]; Menno Kappers[1]; Colin Humphreys[1]; [1]University of Cambridge

It is presently unclear whether threading dislocations (TDs) in heteroepitaxial GaN films arise at island coalescence boundaries or in the initial film nucleation layer. To resolve this question, we studied a series of GaN films with thicknesses ranging from the nucleation layer to 500 nm. The TD densities and the degree of film coalescence were studied using cathodoluminescence, scanning electron microscopy, X-ray diffraction and atomic force microscopy. The density of a-type TDs at the film surface first decreases, then increases, whereas the density of (a+c)-type TDs increases slightly as the film coalesces. Although some TDs appear as the films coalesce, at least ~ 80% of TDs are present at the very start of growth and cannot appear due to island coalescence. X-ray diffraction data show that the initial islands are not misoriented by tilt and we conclude that TDs are instead predominantly formed in the GaN nucleation layer.

11:45 AM

Electron Beam Induced Current Contrast of Threading Edge Dislocation in n-Type 4H-SiC Epilayers: *Ronen Berechman*[1]; Marek Skowronski[1]; [1]Carnegie Mellon University

Contrast of threading dislocations in 4H-SiC Schottky diodes was measured by Electron Beam Induced Current method (EBIC) as a function of the n-type background doping density. The doping concentrations were between $4.6x10^{14}$ cm^{-3} and $7.2x10^{16}$ cm^{-3} with the corresponding contrast change between 3% and 17 %. Donolato's expression for the recombination strength and the calculated minority carrier density within the dislocations space charge region were used to find the recombination rates. The recombination rate increased linearly with doping density. This result was interpreted within the framework of the Shockley-Read-Hall recombination statistics. The height of upward band bending at the dislocation, caused by the capture of electrons by bandgap traps in the dislocation core, and the trap level were extracted.

12:00 PM

Dislocations in Si-Doped LEC GaAs Revisited: A Spectrum Image Cathodoluminescence Study: Oscar Martínez[1]; *Juan Jiménez*[1]; [1]University of Valladolid

Understanding the role of impurities is crucial to semiconductor device technology. The incorporation of these impurities to the lattice and the resulting free charge concentration depend on the interaction with native defects. Dislocations in Si-doped substrates were studied in the nineties using highly sensitive Diluted Sirtl applied with Light etching, Electron Beam Induced Current and micro-Photoluminescence techniques, aiming to understand the interaction between dislocations and the doped GaAs matrix. CL spectrum imaging allows revisiting this problem. By using a CCD multichannel detector it is possible to obtain the full spectral information over a selected area with submicrometric spatial resolution. The local spectra allow the identification of the defects responsible for the luminescence emission. The use of fitting routines allows mapping the distribution of the different defects and impurities, providing a full scenario of the Cottrell atmosphere. The CL images are complemented with etching depth images obtained by Phase Stepping Microscopy.

12:15 PM

Determination of Piezoelectric Fields across InGaN/GaN Quantum Wells by Means of Electron Holography: Masashi Deguchi[1]; *Shigeyasu Tanaka*[2]; Takayoshi Tanji[2]; [1]Department of Electronics, Nagoya University; [2]EcoTopia Science Institute, Nagoya University

Electron holography (EH) was used to determine the piezoelectric fields across an InGaN/GaN quantum well structure in commercially available blue light emitting diodes. A wedge polishing technique was used for thinning samples. Thin samples prepared by this technique had wedge fronts nearly perpendicular to the interface, thus suitable for EH analysis. Holograms were taken under the condition that the sample was tilted such that the adjacent layers slightly overlapped. The tilting of the samples helps to avoid strong diffraction effects which cause an additional phase shift and make the analysis difficult. The phase changes in the overlapped regions were analyzed to determine the piezoelectric fields in each well. It was shown that the piezoelectric field is strongest at the center region of the quantum well structure. The field strength averaged over eight InGaN wells was approximately 2.2 MV/cm.

Industrial Instrumentation

Monday PM Room: Glessner Auditorium
September 14, 2009 Location: Oglebay Resort & Conference Center

Session Chair: Robert Stahlbush, Naval Research Laboratory

1:30 PM
The Ability to Obtain TEM Image without Aberrations and Delocalization - What Does this Mean for Imaging at the Atomic Scale?: *J. Ringnalda*[1]; [1]FEI Company

2:10 PM
Optical and Infrared Microscopy for Locating and Characterizing Defects in Semiconductor Materials and Devices: *J. McDonald*[1]; [1]Quantum Focus Instrument Corp.

2:50 PM
Wafer-Scale Noncontact Imaging of Electrical Defects for Photovoltaics and IC Applications: *C. Moore*[1]; [1]Semilab USA

Poster Session

Mon, 4:30-7:00 PM Room: Banquet Rooms 1-3
September 14, 2009 Location: Oglebay Resort & Conference Center

A Non-Destructive UVPL Examination of Electric Fields in Termination Regions of 4H-SiC Devices: *Marko Tadjer*[1]; Kendrick Liu[2]; Robert Stahlbush[2]; Karl Hobart[2]; Mario Ancona[2]; Fritz Kub[2]; [1]University of Maryland; [2]Naval Research Laboratory

Efficient electric field termination is of paramount importance for the stable operation of high power electronic devices. A non-destructive technique for characterization of the electric field in termination region of 4H-SiC power devices is presented. A 4H-SiC diode, provided by CREE Inc. with a guard-ring termination was used in this work. The carrier concentration level of 8x1014 cm-3 was measured using a capacitance-voltage technique and the effect of the guard rings on the hole current density was simulated using drift-diffusion theory. The concentration of UV-generated carriers under the guard rings was monitored by photoluminescence (PL). The reverse bias field, varied up to 1 kV, depleted the photo-generated carriers and thus reduced the radiative recombination. This effect produced a contrast in the PL image, which delineated the edge of the space charge region along the radius of the guard rings.

Accelerated Light Induced Degradation, ALID, for Monitoring of Defects in PV Silicon Wafers and Solar Cells: Marshall Wilson[1]; *Piotr Edelman*[1]; Alexandre Savtchouk[1]; John D'Amico[1]; Jacek Lagowski[1]; [1]SemilabSDI

In crystalline silicon, above bandgap illumination can transform iron and boron-oxygen from weak recombination centers into strong recombination centers, causing light induced degradation of minority carrier lifetime and corresponding degradation of solar cell efficiency. This process can be reversed using thermal treatments that are distinctly different for iron and for boron-oxygen defects. Combining illumination and thermal treatment, we have designed an accelerated light induced degradation cycle. It has three distinct stages needed to isolate individual contributions to lifetime from interstitial iron Fe_i and boron-oxygen dimer ($B\text{-}O_{2i}$). With this cycle, the concentration of Fe_i and $B\text{-}O_{2i}$ is determined using SPV diffusion length measurement. Wafer scale SPV mapping is used to differentiate between the spacial distribution of $B\text{-}O_{2i}$ and Fe_i in PV wafers and final solar cells. This new ALID, enables complete solar cell degradation in minutes as compared to 24 to 48 hours of light soaking used in previous LID monitoring.

Band Gap States in AlGaN/GaN Hetero-Interface Studied by Deep-Level Optical Spectroscopy: *Yoshitaka Nakano*[1]; Keiji Nakamura[1]; Yoshihiro Irokawa[2]; Masaki Takeguchi[2]; [1]Chubu University; [2]National Institute for Materials Science

We have investigated band gap states in $Al_{0.3}GaN/GaN$ hetero-structure grown on sapphire substrate, employing capacitance-voltage (C-V) and capacitance deep-level optical spectroscopy (DLOS) techniques. Compared the photo C-V characteristics ($\lambda > 390$ nm) to the dark C-V ones, an increased concentration Δn_s of the 2DEG on illumination is estimated to be at least ~$1.8x10^{11}$ cm^{-2} and is considered to be optically excited from deep-level defects to the 2DEG at the AlGaN/GaN hetero-interface. From DLOS measurements, two specific deep levels are revealed to be located at ~1.70 and ~2.08 eV below the conduction band, being clearly different from the deep-level defects observed in GaN. Both deep levels show a significant increase in their corresponding steady-state photo-capacitance in partial pinch-off mode. Therefore, these levels probably stem from the 2DEG region at the AlGaN/GaN hetero-interface. In particular, the 1.70 eV level is likely to act as an efficient trap center for 2DEG carriers.

Capacitance Spectroscopy of Deep States in Quantum Dot Heterostructures: *Mikhail Sobolev*[1]; [1]Ioffe Physical-Technical Institute of the Russian Academy of Sciences

Using capacitance-voltage and deep-level transient spectroscopy (DLTS), we previously showed that the electrical properties InAs/GaAs heterostructures with VCQDs are strongly affected by the interaction between the carriers localized in QDs and the surrounding point defects. We discovered (i) the Coulomb interaction between charge carriers localized in the QDs with ionized point defects; and (ii) Metastable population of quantum states in the QDs, achieved by isochronal annealing and bias-on-bias-off cooling conditions and white light illumination. Moreover, we showed that there are the following effects in heterostructures with vertically coupled QDs: (i) Stark effect in quantum-dot molecule, and (ii) Wannier-Stark effect in quantum dot superlattices. The manifestation of either of the above effects is related to the variations in the behavior of the DLTS spectra, which allow a distinctive feature of spatially localized states, as compared with deep levels of defects distributed over the bulk of the semiconductor.

Carrier Lifetime Measurements of Semiconductors by Contactless Capacitance-Frequency Method: *Hidenobu Mori*[1]; Haruhiko Yoshida[1]; [1]University of Hyogo

Carrier lifetime measurements of Si wafers contaminated with heavy metal impurity have been carried out by a contactless capacitance-frequency (C-f) method. The heavy metal impurity is very detrimental to semiconductor devices because of shortening carrier lifetime. Carrier lifetime measurements are very important for the high performance of semiconductor devices. In the C-f method that is one of the carrier lifetime measurements, the carrier lifetime can be evaluated from the break frequency of the C-f characteristics. However, sample devices such as metal-oxide-semiconductor (MOS) devices are required in the C-f method. By contrast, the contactless C-f method using the contactless gate electrode can be performed without conducting the device fabrication processes. In this study, carrier lifetime of a partially Ni-contaminated bulk Si wafer was characterized by the contactless C-f method. The validity of the contactless C-f method was verified by comparing with the results of the conventional C-f method using MOS capacitors.

Cathodoluminescence Investigation of CdSe QD Green Laser Heterostructures: *Alexey Shakhmin*[1]; Irina Sedova[1]; Sergei Sorokin[1]; Maria Zamorynskaya[1]; [1]Ioffe Physical Technical Institute

Green lasers emitting at 520–550 nm are extremely important for many applications. Wide-gap II-VI semiconductor compounds remain the most suitable materials for green lasers with electron beam pumping. The study considered the cathodoluminescence investigation of the laser heterostructures with multilayer CdSe/ZnSe QDs grown pseudomorphically by MBE. The heterostructure contains lower and upper ZnMgSSe cladding layers, and asymmetric ZnSSe/ZnSe superlattice waveguide. The active region consists of CdSe QDs sheets symmetrically embedded in ZnSe QW.The cathodoluminescence was used for studying the internal layers composition as well as the surface layer, the QDs luminescence intensity and time dependence at different electron beam excitation power. The in-depth scanning performed using variation of electron beam energy. The cathodoluminescence was applied for the diagnostics of confinement and carrier transport properties of heterostructures. The cathodoluminescence images revealed the different dislocations density and are correlated with the spectra and transport properties of the structures.

Cathodoluminescence Study of Orientation Patterned GaAs Crystals for Non-Linear Optics: Oscar Martínez[1]; *Juan Jiménez*[1]; [1]University of Valladolid

Orientation patterned (OP)-GaAs crystals are very promising for its use in non-lineal optical applications. Material characteristics concerning the propagation losses, the crystal dimensions and the available periods must be

taken into account to implement the crystal quality. One of the main sources of optical losses is located at the walls between adjacent domains. In this study, OP-GaAs crystals with a total layer thicknesses exceeding 1 mm were grown by hydride vapor phase epitaxy and studied by cathodoluminescence (CL). The periodically reversing of the orientation of the GaAs crystal structure was created using a non-polar Ge layer. The CL studies allow correlating the morphology to the luminescence emission. The domain walls were non radiative recombination regions, due to the antibonds, though other defects were observed to inhibit partially their non radiative recombination activity. The domain walls were decorated by point defects, which are sources of compressive stress around the domain walls.

Chalcopyrite Heterojunction Photovoltaic Devices: *Okechukwu Akpa*[1]; Shoieb Shaik[1]; Kalyan Das[1]; [1]Tuskegee University

Films of $CuInSe_2$ and $CuGaSe_2$ were deposited on (100) Si. The growth procedure involved r.f. magnetron sputtering. Electrical measurements indicated that the grown films were p-type and formed an abrupt p-n junction with Si. Rutherford back scattering (RBS) data yielded a composition of $Cu_{1.05}In_{1.04}Se_{2.5}$ for $CuInSe_2$ which indicates that near-stochiometric films were obtained. However, the composition of $Cu_{1.0}Ga_{3.0}Se_{0.6}$ for $CuGaSe_2$ shows Ga rich and Se poor layers. Circular geometry diodes with diameters between 100-400 µm, were fabricated on the $CuInSe_2$ and $CuGaSe_2$ films with a common Au back contact. The forward bias current increased by three orders of magnitude when illuminated by a 75 W halogen lamp. This indicates that a p-n junction with photovoltaic response was formed between the films and Si. The estimated open -circuit voltage VOC for these devices is close to 0.5 - 0.7V.

Characterization of Carrier Lifetime and Surface Recombination Velocity of Semiconductor Wafer by Contactless Zerbst Method: *Shingo Kuge*[1]; Haruhiko Yoshida[1]; [1]University of Hyogo

Contactless Zerbst method has been applied to characterizing carrier lifetime and surface recombination velocity of a semiconductor wafer. In the contactless Zerbst method, the carrier lifetime and the surface recombination velocity can be characterized without the influence of gate leakage current and device fabrication processes. Moreover, the wafer map of the carrier lifetime and the surface recombination velocity can be obtained by scanning a contactless gate electrode on a sample wafer. In this study, carrier lifetime and surface recombination velocity of a partially Au-doped Si wafer were characterized by the contactless Zerbst method. The spatial distributions of the carrier lifetime and the surface recombination velocity were almost in agreement with that of the Au bulk trap density measured by contactless isothermal capacitance transient spectroscopy. The results revealed that the contactless Zerbst method is a powerful tool for characterizing carrier lifetime and surface recombination velocity of a semiconductor wafer.

Characterization of Cu(In,Ga)(S,Se)2 Thin Films Prepared by Sequential Evaporation for Photovoltaic Device Applications: *Toshiyuki Yamaguchi*[1]; Shun Tsumura[1]; Kazuhiro Ohta[1]; Shigetoshi Niiyama[1]; Toshito Imanishi[1]; Kenji Yoshino[1]; [1]Wakayama College of Technology

Cu(In,Ga)(S,Se)2 thin films are one of the promising candidates for absorber materials in single-junction and tandem solar cells. The defects of Cu-Se di-vacancies are formed in Cu(In,Ga)Se2 thin films and influence to the solar cell performance. In this study, we have fabricated Cu(In,Ga)(S,Se)2 thin films by sequential evaporation from CuGaSe2, CuInSe2, In2Se3 and In2S3 compounds for photovoltaic device applications and their properties have been investigated. From XRF and EPMA analysis, the S/(S+Se) mole ratio in the thin films increased with increasing the In2S3/In2Se3 mole ratio in the evaporation materials. X-ray diffraction studies revealed that the thin films had a chalcopyrite Cu(In,Ga)(S,Se)2 structure and the preferred orientation to the 112 plane. The value of Voc in Cu(In,Ga)(S,Se)2 thin film solar cells increased with increasing the In2S3/In2Se3 mole ratio in the evaporation materials.

Characterization of Ohmic Contacts and Graphene on SiC by Auger Electron Spectroscopy and Raman Mapping: *Mohammad Maneshian*[1]; Nigel Shepherd[1]; [1]University of North Texas

Ti was deposited by pulsed laser deposition onto SiC, and the structures annealed at temperatures ranging from 950 to 1450ºC in the vacuum of 10-6 Torr in order to form Ohmic contacts. Anneals at the higher temperatures in the aforementioned range simultaneously produced graphene by sublimation of Si from the SiC, and a pronounced effect on the Ohmic characteristics was observed. Auger electron spectroscopy (AES) was used to investigate lateral and depth-wise diffusion of Ti into the SiC substrate, and Raman spectroscopy was used to monitor the extent of graphene formation after different annealing stages.

Comparative Study of Heteroepitaxial Domain Growth Mg0.4Zn0.6O Alloy Films on LaAlO3 and MgO Substrates: *Lin Zhuang*[1]; K. H. Wong[2]; H. Shen[1]; [1]Sun Yat-sen University; [2]The Hong Kong Polytechnic University

Cubic phase heteroepitaxial domain Mg0.4Zn0.6O films have been realized on both LaAlO3 (100) and MgO (100) substrates using pulsed laser deposition. Different domain matching epitaxy relationships were obtained due to the different lattice mismatch between the films and substrates. A 45° rotated diagonal domain growth (2 diagonal units of Mg0.4Zn0.6O to 3 units of LAO) results in a mismatch of less than 2%. While perfectly matched cube-on-cube relationship is demonstrated in the Mg0.4Zn0.6O/MgO structure. X-ray diffraction confirms that substrates have little effects on the lattice parameters of the Mg0.4Zn0.6O films.

Controlled Electron Beam Irradiation Effect on the Transport and Optical Properties of Undoped ZnO Single-Crystal: Filippo Fabbri[1]; *Benjamin Dierre*[2]; Nicola Armani[1]; Giancarlo Salviati[1]; Xiaoli Yuan[2]; Takashi Sekiguchi[2]; [1]IMEM-CNR; [2]Advanced Electronic Materials Center, National Institute for Materials Science

Controlled electron beam irradiation can give an insight on the optical and transport properties of ZnO devices. Non-intentionally doped ZnO single-crystals usually show slightly n-type behavior due to impurity-related shallow donors, responsible for the dominant ultraviolet emission found by optical characterizations. A detailed study of e-beam irradiation experiments at different injection power conditions on the evolution of the I-V characteristics is presented. Un-irradiated samples show slightly rectifying properties. After 1-hr of irradiation a rectifying-to-ohmic transition occurs and the sample current increases. Simultaneous cathodoluminescence characterization reveals strong degradation of the UV luminescence. A partial decrease of the current occurs when the e-beam is stopped and the sample is exposed to air, while the ohmic behavior is maintained. These results suggest a serious change of the concentration of shallow donors, responsible for the slightly n-type and of the UV emission, and the (de-)activation of centers due to point-defect complexes.

Dependence of Ag/In Ratio of $AgInS_2$ Crystals Grown by Hot-Press Method: *Takahiro Tokuda*[1]; Akira Nagaoka[1]; Kenji Yoshino[1]; [1]University of Miyazaki

$AgInS_2$ crystals with changing Ag/In ratio were grown by a Hot-Press method at 700°C under 25 MPa for 1 hour. The size of all samples was 20 mm in diameter. The samples were evaluated X-ray diffraction (XRD), electron probe micro analysis (EPMA), density and Hall measurements. From the XRD spectra, $AgIn_5S_8$ phases were observed in In-rich samples, respectively. Furthermore, lattice constants of In- and Ag-rich were larger than those of stoichiometric sample. It is assumed that this is due to exist interstitial atoms. Density become large with increasing Ag/In ratio. From Hall measurement, all samples indicate n-type conductivity. It is deduced that lattice defects of interstitial Ag atoms and sulphur vacancy are existed in Ag- and In-rich samples, respectively.

Detailed Analysis of Temperature Characteristics of InGaP/InGaAs/Ge Triple-Junction Solar Cell: *Kensuke Nishioka*[1]; Tsuyoshi Sueto[1]; Masaki Uchida[1]; Yasuyuki Ota[1]; [1]University of Miyazaki

Temperature characteristics of InGaP/InGaAs/Ge triple-junction solar cell were analyzed in detail using equivalent circuit calculation. The current-voltage (I-V) characteristics of single-junction solar cells (InGaP, InGaAs, Ge solar cells) were measured at various temperatures. The structures of the single-junction solar cells have striking resemblance to those of each junction in the InGaP/InGaAs/Ge triple-junction solar cell. The fitting of I-V curves between measured and calculated data were carried out, and the diode parameters and temperature exponents of the single-junction solar cells were extracted. The parameters for each single-junction solar cell were used in the equivalent circuit model for InGaP/InGaAs/Ge triple-junction solar cell, and the calculations of solar cell performance were carried out. Measured and calculated results of the illuminated I-V characteristics of triple-junction solar cell at various temperatures from 30 to 100°C agreed well. By using this method, the performance of triple-junction solar cells at various temperatures can be estimated accurately.

Effect of Al Doping on Morphology of ZnO Films Prepared by Spray Pyrolysis: *Chanchana Thanachayanont*[1]; Yot Boontongkong[1]; Chanipat Euvananont[1]; [1]National Metal and Materials Technology Center

ZnO films have been prepared by the spray pyrolysis method using 0.05M solution of zinc acetate dihydrate in methanol as the precursor. The films were grown at 430°C for 2.5 hrs, with Al doping achieved by the addition of AlCl3. The ZnO film morphology was found to evolve from a relatively dense structure comprising hexagonal platelets in the undoped film, towards a more porous structure comprising faceted particles with increasing AlCl3 doping to 2.5%. The film doped with 2.5% AlCl3 exhibits a microstructure not observed in the undoped sample. The morphology comprises clearly faceted particles of size 250 to 500 nm, which are larger than the hexagonal platelets seen in the undoped film. The existence of the well-faceted particles can be attributed to the presence of HCl during film formation which leads to the predominance of the {101} forms in ZnO crystals, which then results in well-faceted pyramidal particles.

Effect of Non-Stoichiometry on Point Defect Levels in 6H-SiC Single Crystals: Pawel Kaminski[1]; *Michal Kozubal*[1]; Katarzyna Racka-Dzietko[1]; Krzysztof Grasza[1]; Emil Tymicki[1]; Stanislaw Warchol[2]; [1]Institute of Electronic Materials Technology; [2]Institute of Nuclear Chemistry and Technology

Deep-level transient spectroscopy (DLTS) was used to study electronic properties of non-stoichiometry-related defect centres in 6H-SiC bulk crystals grown by physical vapour transport (PVT). In the as-grown C-rich crystals, five electron traps labeled as T1A, T1B, T2, T3 and T4 with activation energies 0.34, 0.40, 0.64, 0.67 and 0.69 eV, respectively, were revealed. After the irradiation with a dose of ~$2x10^{17}$ cm^{-2} of 0.3-MeV electrons, a new electron trap T1C (0.50 eV) was formed. In the as-grown Si-rich crystals, only the traps T1A and T1B were found. An effect of the energy of bombarding electrons on the formation of traps T1A, T1B, T1C, T2, T3 and T4 was observed. At the energy of 0.3 MeV, the traps T1A and T1B were found to be predominant. At the energy of 0.7 MeV, the predominant traps were T2 and T3 and at the energy of 1.5 MeV the predominant trap was T1C.

Effect on Ordering of the Growth of GaInP Layers on Polar and Non Polar GaAs Faces: Oscar Martínez[1]; *Juan Jiménez*[1]; [1]University of Valladolid

GaInP is an essential material for multijunction structures of III-V compounds for solar cells. The growth of GaInP on polar GaAs faces could achieve better photovoltaic responses, the large internal electric fields generated by the off-diagonal strain could allow for a better extraction of minority carriers and the suppression of long range order. We explored here the growth by MOCVD of GaInP layers on (001), (111)Ga and (111)As - GaAs substrates. Three different flows of Phosphine (290, 320 and 350 sccm/min) were used, keeping all the other growth parameters constant. The structural and optical properties of the different layers have been studied by SIMS, X-Ray, μRaman, μPL and CL. It has been observed that a completely disordered alloy can be obtained when growing onto polar surfaces. Some other problems as the control of composition and the diminution of the growth rate are addressed.

Electrical and Optical Characteristics of Electron Irradiated Gallium Oxide Films Grown by RF Magnetron Sputtering: *Kenichiro Takakura*[1]; Tomohiro Kudou[1]; Kiyoteru Hayama[1]; Masashi Yoneoka[1]; Hidenori Ohyama[1]; Mutsuo Shibuya[2]; Yoshio Kayamoto[3]; [1]Kumamoto National College of Technology; [2]Japan Gas Chemi; [3]Koto Manufactureing

Up to now, indium oxide (ITO) is mainly used as transparent electrode material for e.g. solar cell applications. Drawbacks are the toxicity and limited supply of the material. Gallium oxide is expected to be a promising alternative as transparent electrode material. It is a wide band gap semiconductor (4.9 eV) and un-doped gallium oxide film becomes n-type when sufficient oxygen vacancies are formed. Therefore, it is considered to increase the carrier density by electron irradiation of gallium oxide. We have grown gallium oxide films by sputtering, and electrical and optical characteristics of the films that were electron irradiated have been studied. To investigate the resistivity of the films, ohmic contact are fabricated, using Ti electrodes. It is shown that the resistivity of the films decreases with increasing electron fluence. Also, the sub band gap optical absorption coefficient increased by the irradiation. These results suggest that the irradiation is effective to decrease resistivity of the gallium oxide film.

Electron Scattering Mechanism of FTO Films Grown by Spray Pyrolysis Method: *Minoru Oshima*[1]; Kenji Yoshino[1]; [1]University of Miyazaki

F-doped SnO_2 (FTO) films have attracted much attention as transparent conductive oxide material. The spray pyrolysis method is effective for thin film growth because no plasma damages of a substrate, no high vacuum and low costs of equipment have in the growth technique. The FTO poly films were successfully grown by spray pyrolysis method at 350 ~ 500°C. High transmittances (85%~) and low resistivities (~ 8×10^{-4} Ωcm) could be obtained [1]. Electron scattering mechanism of FTO films is examined from the results of Hall measurements. From calculation of the average free pass of electron, it is found that ionization impurity scattering of electron is dominant in this film. At the same time, the neutral impurity scattering of electron disturbs the low resistivity of the sample.[1] M. Oshima, Y. Takemoto, K. Yoshino, Physica Status Solidi (C) (2009) accepted

Electron Scattering on the Short-Range Potential of the Crystal Defects in ZnHgSe and ZnHgTe Solid Solutions: *Orest Malyk*[1]; [1]Lviv Polytechnic National University

In the present paper the short-range principle for description of the electron scattering in ZnHgSe and ZnHgTe solid solutions is used. For the electron scattering on nonpolar optical and acoustic phonons, neutral defects , disorder and static strain potential the interaction radius of the short-range potential is limited by one unit cell. For the electron scattering on the ionized impurity, polar optical and piezoelectric (piezoacoustic and piezooptic) phonons the interaction radius of the short-range potential is founded in a form $R=\gamma a$ (a - lattice constant, γ – the respective adjusting parameters). To calculate the conductivity tensor components the method of a precise solution of the stationary Boltzmann equation was used. The temperature dependences of the electron mobility in the range 4.2 – 370 K in $Zn_xHg_{1-x}Se$ (0.02=x=1) and $Zn_xHg_{1-x}Te$ (x=0.15) crystals are calculated. The influence of the different scattering mechanisms on the electron mobility is considered.

Enhancement of Defect Production Rates in n-Type Silicon by Hydrogen Implantation at around 270 K: *Yutaka Tokuda*[1]; Youichi Nagae[1]; Hitoshi Sakane[2]; Jyoji Ito[2]; [1]Aichi Institute of Technology; [2]S.H.I. Examination & Inspection Ltd.

We have discovered the introduction of metastable defects in n-type silicon implanted with hydrogen at 88 K and subsequently heated to room temperature in addition to vacancy-related and hydrogen-related defects. In this work, we have studied the production behaviour of these defects by varying the implantation temperature in the range from 88 to 303 K. Samples prepared from n-type (100) CZ wafers with a resistivity of 1 – 2 Ocm were implanted with 100 keV hydrogen ions at a dose of $2x10^{10}$ cm^{-2}. DLTS measurements were performed for fabricated Schottky diodes. We have found that the production rates of defects are greatly enhanced by hydrogen implantation in the range from 260 to 280 K. Such peculiar defect production behaviour was not observed in He-implanted samples. It is suggested that hydrogen plays an important role in enhancement of defect production rates in hydrogen-implanted n-type silicon at around 270 K.

EPR Study of Diluted Magnetic Semiconductors $Ge_{1-x}Mn_xTe$: *Elena Zvereva*[1]; Olga Savelieva[1]; Valentina Akishina[1]; Evgeny Skipetrov[1]; Evgeny Slyn'ko[2]; Vasily Slyn'ko[2]; [1]Moscow State University; [2]Institute of Material Science Problems

We have performed electron paramagnetic resonance (EPR) measurements in diluted magnetic semiconductors $Ge_{1-x}Mn_xTe$(x=0.1-0.5) at 9.6 GHz between 80 and 400 K. Excellent agreement between theoretical and experimental data has been achieved assuming a superposition of two Dysonian type lines (narrow one with $\Delta H_1 \approx 250 \pm 50$ Oe and $g_1 \approx 1.98 \pm 0.01$, and wide one with $\Delta H_2 \approx 1400 \pm 100$ Oe and $g_2 \approx 2.02 \pm 0.01$ at room temperature) in the derivative of the power absorbed. The linewidth of narrow line remains practically unchanged under variation of manganese content, while it increases with increasing of Mn content for wide one. Temperature dependencies of linewidths and effective g-factor revealed an anomaly in the vicinity of the ferromagnetic ordering temperature. Broadening of linewidth with lowering the temperature was observed and satisfactory described in the frame of modified Huber model. Estimations of ferromagnetic ordering temperature and paramagnetic Curie-Weiss temperature are found to be in reasonable agreement with the values determined from magnetic measurements.

Evaluation of Strain and Crystal Quality in Si during Shallow Trench Isolation Process Using UV-Raman Spectroscopy: *Daisuke Kosemura*[1]; Yoshida Tetsuya[1]; Maki Hattori[1]; Toshikazu Mizukoshi[2]; Atsushi Ogura[1]; [1]Meiji University; [2]Oki Semiconductor Co., Ltd.

Shallow trench isolation (STI) technique is used for an electrical separation between devices in LSI. It is concerned that defects and strain are induced in Si during STI process. We evaluated strain and crystal quality in Si during STI process using UV-Raman spectroscopy. Parts of the STI processes including trench etching, liner oxidation, and annealing were evaluated. The annealing condition was at 1150°C for 4, 6, and 8 hr. In UV-Raman measurements, the surface sensitivity is excellent because the penetration depth of UV-laser is about 5 nm. Trench etching induced compressive strain and degradation of crystal quality detected by the high wave-number shift and increase of FWHM. Furthermore, the liner oxidation induced more compressive strain. After annealing, strain relaxation and recovery of crystallinity were confirmed. However, FWHMs of Raman spectra were different between the centre and edge of wafer, which indicates the chip-to-chip fluctuation of crystal quality in Si.

Evolution of Optical and Mechanical Properties of Semiconductors over 40 Years: *Sergei Pyshkin*[1]; John Ballato[2]; [1]Academy of Sciences; [2]Clemson University

We discuss over 40 years evolution of optical (luminescence, light absorption and Raman scattering) and mechanical (microhardness) properties of the group of single crystals including representatives of the mono-atomic, binary and ternary semiconductors. We show that the long-term natural stimuli improving perfection of the grown in laboratory conditions crystals prevail over the others which could lead to heterogenic systems. Systematic monitoring proves that the long-term diffusion and stress relaxation processes lead to the host atoms being placed in their proper equilibrium positions and to a more uniform redistribution of the impurities or structural defects. We demonstrate that highly ordered nature of this new crystal lattice facilitates stimulated emission, increases the radiative recombination efficiency of electron–hole pairs and spectral range of luminescence equally at low and at room temperatures. It means that new ways for fabrication of semiconductor devices with high and stable in time characteristics really do exist.

Fluorine Induced Twinned Crystalline SnO2 Thin Films: *Chanchana Thanachayanont*[1]; Chanipat Euvananont[1]; [1]National Metal and Materials Technology Center

Thin films of tin oxide (SnO2) were prepared by spray pyrolysis technique. The SnO2 suspensions were obtained from of SnCl2 in 90% of methanol and 10% of DI water. Fluorine doping was achieved by adding NH4F. Fluorine doping concentration was varied having F:Sn molar ratios of 0:1, 0.5:1 and 1:1, respectively. Deposition temperatures of 300, 400 and 500°C were investigated. Average grain size and film thickness were found to increase with an increase in deposition temperature (from 300°C to 500°C) and with an increase in F doping concentration from 0:1 to 1:1 F:Sn molar ratio. The lowest sheet resistance of 1.86 Ohm/square was observed on the 1:1 F:Sn molar ratio sample deposited at 500°C. Despite a decrease in resistivity with an increase in fluorine doping, twinned crystals were observed in the 1:1 F:Sn molar ratio indicating imperfect substitution of the fluorine atoms on the tin lattice sites.

Growth and Characterization of $CuInTe_2$ Crystals Grown by Hot-Press Method: *Ryuichi Tashiro*[1]; Akira Nagaoka[1]; Kenji Yoshino[1]; [1]University of Miyazaki

Undoped $CuInTe_2$ crystals were grown by hot-press (HP) method at 400 ~ 700°C for 1 h under high pressure (10 ~ 40 MPa). One of the advantages of the HP method is that a crystal growth is easy at low temperature. $CuInS_2$ and $AgInS_2$ crystals could be successfully grown by the HP method in our previous work. The sizes of the samples were 20 mm in diameter. All samples indicate chalcopyrite structures, nearly stoichiometry and p-type by means of X-ray diffraction, electron probe microanalysis and thermoprobe analysis, respectively. However, the sample grown at 400°C has a secondary phase. According to increasing temperature, the sample does not have the secondary phase. A single phase $CuInTe_2$ crystal can be successfully obtained at 600°C. This temperature is lower than the melting point.

Growth and Characterization of $IrSnO_x$ Films Grown by Sputtering Method: *Syun Harada*[1]; Kenji Yoshino[1]; [1]University of Miyazaki

$IrSnO_x$ thin film which is respected as electrochromic on glass substrate was obtained at room temperature with changing base pressure (2 ~5 Pa) using 2 kinds of SnO_2 and iridium targets. All samples indicate amorphous by XRD spectra. Thickness of the samples decreases slightly with increasing base pressure. Optical transmittance decreases with increasing the pressure. Furthermore, their refractive index increase with increasing the pressure. These results indicate that iridium ratio in the film increases with increasing the pressure. An electrical resistivity decreases with increasing the pressure. This means that the electrical resistivity decreases with increasing iridium concentration. It is assumed that one of this increasing of the electrical resistivity may be due to increasing an oxygen vacancy by XPS results.

Growth and Photoluminescence of $AgGaSe_2$ Crystals Grown by Hot-Press Method: *Akira Nagaoka*[1]; Kenji Yoshino[1]; [1]University of Miyazaki

Undoped $AgGaSe_2$ crystals are grown by hot-press (HP) method at 400 ~ 700°C for 1 h under high pressure (10 ~ 40 MPa). One of the advantages of the HP method is that a crystal growth is easy at low temperature. $CuInS_2$ and $AgInS_2$ crystals could be successfully grown by the HP method in our previous work. The sizes of the samples are 20 mm in diameter. All samples indicate chalcopyrite structures, nearly stoichiometry and n-type by means of X-ray diffraction, electron probe microanalysis and thermoprobe analysis, respectively. However, the sample grown at 400°C has a secondary phase. According to increasing temperature, the sample does not have the secondary phase. A single phase $AgGaSe_2$ crystal can be successfully obtained at 700°C. Furthermore, the $AgGaSe_2$ crystal is high quality because a free exciton emission is clearly observed in the photoluminescence at low temperature.

Imaging and Modeling Diffusion to Isolated Defects in a GaAs/GaInP Heterostructure: *Tim Gfroerer*[1]; Mac Read[1]; Mark Wanlass[2]; [1]Davidson College Physics Department; [2]National Renewable Energy Laboratory

Defect-related electron-hole pair recombination impairs the performance of many semiconductor devices. In photoluminescence images, defective regions appear dark because carriers are more likely to recombine nonradiatively. We use photoluminescence imaging to observe isolated defects in a GaAs/GaInP heterostructure. We find that the area of the defect-darkened region depends strongly on the photoexcitation intensity. With increasing excitation, the density of electrons and holes increases, so they are more likely to encounter each other and recombine radiatively before reaching the defect. We model the behavior with a computer simulation that allows for lifetime-limited Laplacian diffusion of carriers, and we report good qualitative agreement between the experimental and simulated images. We are currently developing a more sophisticated model in hopes of achieving better quantitative agreement.

Imaging Inhomogenities Doping in HVPE Grown GaN with Kelvin Probe Microscopy and Photoetching: *Grzegorz Nowak*[1]; J. L. Weyher[1]; B. Lucznik[1]; I. Grzegory[1]; [1]Institute of High Pressure Physics, Polish Academy of Sciences

Thick HVPE GaN layers grown on top of GaN on sapphire substrates were investigated. Such layers initially grow in form of separate pyramids, which are later overgrown creating flat crystallization front. In-plain surface potential was generally uniform with distinct non-uniform islands. Every such region had characteristic border with lower potential indicating higher doping level. Cross-sectional KPFM images revealed series of dome-like lines of lower potential. Distribution of surface potential was uniform outside of the lines and non-uniform inside. KPFM images were compared to and shown good correlation with those obtained with photo-enhanced chemical etching. Measured surface potential maps indicated that impurities are incorporated preferentially at sides of the growth pyramids leading to higher local electron concentration. Between and above the pyramids surface potential is uniform indicating uniform doping with lower electron concentration.

Imaging the Catastrophic Optical Mirror Damage in High-Power Diode Lasers: *Mathias Ziegler*[1]; Jens Tomm[1]; Thomas Elsaesser[1]; Ute Zeimer[2]; [1]Max-Born-Institut; [2]Ferdinand-Braun-Institut für Höchstfrequenztechnik

We report on the combination of thermography and near-field imaging for monitoring the catastrophic optical mirror damage (COMD) of red- and infrared-emitting high-power broad-area diode lasers operating in cw and single-pulse mode. Thermography is highly COMD-selective since it has the unique capability of directly imaging the abrupt threshold-like device-temperature increase during

the thermal runaway and subsequent melting processes, appearing as a "thermal flash". From monitoring the near-field pattern we can anticipate potential COMD locations and follow the damage-induced loss in laser intensity. Additional analysis with scanning-electron microscopy and cathodoluminescence links to the COMD-induced structural changes at the facet and in the volume. All techniques exhibit strong correlations in COMD location and strength, and, because of the thermal flash, allow for an unambiguous decision about the COMD occurrence, also in situations of competing degradation mechanisms. Applied in concert, the approach enables for deeper insight into the physics behind COMD.

In-situ Observation of Strain Relaxation in Si/SiGe Heterostructure on SOI: *Tongda Ma*[1]; Hailing Tu[1]; [1]General Research Institute for Nonferrous Metals

In order to in-situ observe the strain relaxation, the cross-sectional silicon layer and silicon germanium layer on silicon-on-insulator (Si/SiGe/SOI) was heated from room temperature (R.T.) up to 840°C in ultra-high voltage transmission electron microscope (UHVTEM). Some of the misfit dislocations at the interface between the SiGe layer and the top Si layer of SOI (the middle interface) extended down to the interface between the top Si layer and the buried oxide layer of SOI (the lower interface). Some other misfit dislocations went upwards and stopped in the SiGe layer. The middle interface took the lead in roughening in comparison with the interface between the Si cap layer and the SiGe layer (the upper interface). The misfit dislocations formed after the upper interface turned seriously rough. The strain relaxation mechanism was discussed in details.

Influence of Grain Boundaries on Multicrystalline Silicon Solar Cells Evaluated by LBIC and Equivalent Circuit Model: *Kensuke Nishioka*[1]; Tsuyoshi Sueto[1]; [1]University of Miyazaki

Influence of grain boundaries on multicrystalline silicon solar cell was evaluated by the laser beam induced current (LBIC) technique and modified 2-diode equivalent circuit model. Electrically active and inactive grain boundaries can be distinguished by the contrast of LBIC images. We evaluated the amount (total length) of active grain boundaries in the multicrystalline silicon solar cells. The current-voltage (I-V) characteristics were analyzed by a modified 2-diode equivalent circuit model. By using this model, we can calculate I-V characteristics of solar cells considering diffusion and recombination currents separately, and we can obtain the ratio of recombination area in which the recombination of minority carriers is pronounced. We investigated the relationship between the amount of active grain boundaries and the ratio of recombination area. It was clearly found that the ratio of recombination area increased with increasing the amount of grain boundaries.

Investigation of Electronic Property in CZ-Si with Low Electron Irradiation Dose: *Guifeng Chen*[1]; Xiaowei Ma[1]; Yangxian Li[1]; [1]Hebei University of Technology

The electronic properties in CZ-Si with low electron irradiation dose were investigated with Hall testing instrument and Fourier Transform Infrared Spectrometer (FTIR) at room temperature. It is found that the resistivity of silicon with electron irradiation increased rapid, carrier concentration and mobility ratio declined simultaneity. After these samples annealed under different temperature, the resistivity fallen, the carrier concentration and mobility ratio increased, each parameter resumed ultimately at 400°, the IR absorption peak of A2 samples annealed at different temperature also firmed that the defects introduced electron irradiation eliminated at this temperature. The value of every parameter up to extremum due to the exit of thermal donor at 450°, the crystal lattice resumed to the integrity at 600°.

Key Role of Point and Extended Defects in Plasticity and Fracture of Semiconductors: *Valery Kisel*[1]; [1]Institute of Solid State Physics, Russian Academy of Science

A remarkable finding of this work is the unity of mechanisms of deformation modes motion and multiplication up to nanostructured state and fracture in elemental (Si) and compound (InSb, GaAs) semiconductors under continuous (creep) and interrupted (fatigue) shear stresses τ, magnetic field H in a wide temperature range (T=4.2 to 700K). A mean path length l of deformation modes (dislocations, fracture cracks, etc) changes synchronously with the their mean number n (τ,dτ/dt,T,H), but part of dislocations moves back after the external force, and l,n depend non-monotonously on the frequency of loadings, f, and gradually reach the ultimate values to begin the multiplication. The deformation drag is more prominent for smaller stresses, lowest T and dτ/dt and is determined by the dislocation double cross slip and jog drag/slip around the lattice defects. The scaling of stresses to move/multiplicate of defects confirms this.

LBIC and Reflectance Mapping of Microcrystalline Si Solar Cells: Benito Moralejo[1]; Miguel Gonzalez[1]; *Juan Jiménez*[1]; Vicente Parra[2]; Oscar Martinez[1]; Raquel Descalzo[2]; Javier Gutierrez[2]; [1]Universidad de Valladolid; [2]Instalaciones Pevafersa S.L., Energías Renovables

Multicrystalline Silicon (mc-Si) is increasingly used in the photovoltaic (PV) industry. However, this material is characterized by an intrinsic structural heterogeneity (dislocations, grain boundaries (GB), etc.). The diffusion length of minority gives an indication of material quality and suitability for solar cell use. Laser Beam Induced Current (LBIC) technique allows the estimation of the local diffusion length from photocurrent contrast data. The purpose of this work is to show an advanced homemade LBIC system that highlights the importance of control the laser power excitation and the reflected light, because of the inhomogeneous mc-Si samples. This allows verifying that the minority carrier diffusion length (LDiff), related to the LBIC measurements, is mainly limited by intragrain defects.

Luminescence Enhancement in InGaN and ZnO by Water Vapor Remote Plasma Treatment: *Yoichi Kamiura*[1]; Toshiaki Takenaka[1]; Takeshi Ishiyama[1]; Yousuke Murakami[1]; Chihiro Takenaka[1]; Yoshifumi Yamashita[1]; [1]Graduate School, Okayama University

We have discovered by photoluminescence (PL) spectroscopy at 77 and 300 K that water vapor remote plasma treatment (H_2O RPT) greatly enhances ultraviolet and visible emission from Mg-doped p-type $In_{0.1}Ga_{0.9}N$ films, hydrothermally grown ZnO single crystals and polycrystalline ZnO pellets. The highest enhancing factors were 80 and 240 for $In_{0.1}Ga_{0.9}N$ and ZnO pellets, respectively. We ascribe such enhancing effects to atomic hydrogen that was effectively emitted from water vapor plasma. We have concluded that the blue-green emission from $In_{0.1}Ga_{0.9}N$ is due to the donor-acceptor pair (DAP) recombination mechanism, in which the Mg acceptor doped and a hydrogen-related donor are assumed to act as radiative recombination centers. We ascribe the enhancing effects of H_2O RPT mainly to hydrogen passivation of non-radiative recombination centers and partially to the increased density of a hydrogen-related donor formed particularly in $In_{0.1}Ga_{0.9}N$ by H_2O RPT.

Observation on Defects in Poly-Si Films Prepared by RTCVD under Nonideal Conditions: *Bin Ai*[1]; Hui Shen[1]; Youjun Deng[1]; Chao Liu[1]; Xueqin Liang[1]; [1]Sun Yat-sen University

Polycrystalline silicon (poly-Si) thin films were deposited on quartz substrates by RTCVD (rapid thermal chemical vapor deposition) under nonideal conditions. Crystallographic defects in the poly-Si films were investigated by using TEM. We found that as-deposited poly-Si films contain large quantities of twin crystals including one-order, two-order, three-order and high-order twin crystals. Besides twin crystals, dislocations such as screw dislocation, 60° dislocation, dislocation network, dislocation loop, extended dislocation and dislocation line array were also found. In addition, stacking faults were also observed in as-deposited poly-Si films. Furthermore, the origins of the defects were analyzed, and it was concluded that these defects result from the nonideal deposition conditions and extreme TEM sample fabrication process. Although our experimental results can not really represent the crystallographic quality of poly-Si films prepared by RTCVD, it at least indicates what kinds of defects would exist in poly-Si films when deposited under far-from optimum conditions.

Optical and Electrical Characterization of Annealed Ga-Doped ZnO Films Grown by a Reactive Plasma Deposition: *Yujin Takemoto*[1]; Minoru Oshima[1]; Kenji Yoshino[1]; [1]University of Miyazaki

ZnO is respected as a transparent conductive oxide material as well as ITO (Sn-doped In_2O_3) because of its direct optical bandgap of 3.4 eV at room temperature. In this work, Ga-doped ZnO (GZO) films were deposited on alkali-free glass substrate by ion-plating system with DC arc discharge using a pressure gradient-type plasma gun. In this deposition system, the substrate travelled through the deposition room for the film growth. The GZO films were polycrystalline film with c-axis orientation. Some of the GZO films samples were annealed under air, Ar, O_2 and N_2 atmosphere at from 100 °C to 500 °C. Transmittance and resistivity is drasically changed by O_2 annealing. This indicates that oxygen vacancy is strongly influenced in the GZO film.

PICTS Characterization of Zn Doped Si: *Vladimir Privezentsev*[1]; [1]Institute of Physics & Technology, Russian Academy of Sciences

The Si doped by impurity of double acceptor Zn is traditionally used for development of IR-converters.[1] Recently n-type of such material was investigated by SEM-EBIC method.[2] Have been observed the microdefects with micron size. They have been connected with dislocations or/and zinc precipitates. Now we have investigated Si, doped with phosphorus and then compensated with Zn by PICTS method. Zn impurity concentrations was $N_{Zn}=1x10^{14}cm^{-3}$ and were carried out parity $N_{Zn}<N_p<2N_{Zn}$. After compensation by Zn the electron concentration in Si was $n\tilde{}5x10^{11}cm^{-3}$ (at 300K). In the result of PICTS measurement the activation energy for deep levels 0,55, 0,26, 0,20 and 0,18eV below conductivity zone bottom Ec were revealed. Also the electron capture cross sections for Zn levels in Si were obtained. [1]H. Willebrand, Yu. Astrov, L. Portsel, S. Teperick, T. Gauselmann. IR Phys. Technol., 36, 809 (1995). [2]E.B. Yakimov, V.V. Privezentsev. J. Mater. Sci.: Mater. Electron., 19, S277 (2008).

Structure Analysis of InGaN-Based Light-Emitting Diodes Grown on Patterned Sapphire Substrates and Unpatterned Sapphire Substrates: *Hung-Ling Tsai*[1]; Wei-Chin Li[1]; Jer-Ren Yang[1]; Min -Jang Chen[1]; Makoto Shiojiri[2]; [1]National Taiwan University; [2]Kyoto Institute of Technology

InGaN-based alloy compound semiconductors are useful for optoelectronic devices such as light-emitting diodes (LEDs) in blue and ultraviolet regions. However, due to the large difference in the lattice constant and thermal expansion coefficient, GaN layers grown on sapphire substrate exhibit high dislocation densities. Therefore, how to further reduce the dislocation density is an important issue. In this paper, the InGaN-based blue LEDs were fabricated on patterned sapphire substrate (PSS) and unpatterned sapphire substrate (UPSS) by MOCVD. The quality of the grown GaN epilayers was compared. The microstructure characteristics were investigated by high resolution transmission electron microscope (HRTEM) and high angle annular dark field scanning TEM (HAADF-STEM). From the TEM observations, the PSS was confirmed to be an efficient way to reduce the threading dislocation density and suppress the defect propagation in the GaN epilayer. Finally, better reliability of the PSS LEDs performance was also observed.

Study of Electrical Properties for Electron Irradiated 4H-SiC MESFETs Evaluated by Channel Resistance: *Kenichiro Takakura*[1]; Hidenori Ohyama[1]; Manabu Arai[2]; Satoshi Kuboyama[3]; Sumio Matsuda[3]; [1]Kumamoto National College of Technology; [2]New Japan Radio; [3]JAXA

In this work, we studied the radiation damage in 4H-SiC MESFET. The devices have been irradiated at room temperature with 2-MeV electrons by an electron accelerator. The electron fluence ranged from 1x1013 to 1x1017e/cm2. The electrical characteristics before and after irradiation have been examined to identify the deterioration mechanism. From the current-voltage characteristics, it was derived that the drain current increased with low fluence and decreased at high fluence. In addition, three electron capture levels are observed after irradiation in the DLTS spectra. To verify the sheet resistance in the channel region, the TLM (Transfer Length Method) was performed. The resistance decreased by the electron irradiation because of the increase in the carrier density. The carrier are supplied by nitrogen impurities, with the ionization rate depending on the density in the SiC. The carrier density by irradiation changed the active nitrogen density. In these circumstances, we examined the deterioration mechanism mainly by a change of carrier density.

Tellurium Inclusions and Carrier Trapping Times in Detector Grade Cadmium Zinc Telluride: *Ezzat Elshazly*[1]; Gary Tepper[1]; [1]Virginia Commonwealth University

Carrier trapping times and tellurium inclusions in Cadmium Zinc Telluride (Cd1-xZnxTe, x ~0.1) crystals grown using both the High Pressure Bridgman and Modified Bridgman methods were measured. A pulsed Nd:YAG laser of wavelength 1064nm and a pulse width of 7 ns was used to excite carriers and microwave reflectance was used to probe the carrier trapping time. Infrared microscopy was used to measure the tellurium defect densities in CZT crystals. Tellurium precipitates with diameters = 20 μm were found to be the dominant crystallographic defect. Spatial mapping of carrier trapping times and defect densities in CZT was performed to determine the relationship between defect density and electronic decay. A direct and strong correlation between trapping time and defect density of tellurium inclusions was observed.

Temperature Dependence of Liner Thermal Expansion of $AgGaSe_2$ Crystals: *Akira Nagaoka*[1]; Kenji Yoshino[1]; [1]University of Miyazaki

Undoped $AgGaSe_2$ crystals are grown by hot-press (HP) method at 400 ~ 700°C for 1 h under high pressure (10 ~ 40 MPa). All samples indicate chalcopyrite structures, nearly stoichiometry and n-type by means of X-ray diffraction (XRD), electron probe microanalysis and thermoprobe analysis, respectively. However, the sample grown at 400 °C has a secondary phase. According to increasing temperature, the sample does not have secondary phase. A single phase $AgGaSe_2$ crystal can be successfully obtained at 700 °C. The $AgGaSe_2$ crystal is high quality because a free exciton emission is clearly observed in the photoluminescence at low temperature. Furthermore, temperature dependent XRD and PL are carried out at less than 70 K. A liner thermal expansion decreases and the free exciton peak increases with increasing temperature

The Use of Spatial Analysis Techniques in Defect Studies: *Michelle Moram*[1]; Colin Humphreys[1]; [1]University of Cambridge

Spatial analysis techniques are commonly used by ecologists, biologists, epidemiologists and geographers to analyse spatially varying data. However, although such techniques have the power to reveal underlying spatial correlations and patterns, they have not yet found widespread use in physics. In this work, we show how such techniques can be applied to any experimental data which reveals the positions of crystallographic defects, such as that obtained from atomic force microscopy, transmission electron microscopy, cathodoluminescence microscopy or related techniques. In particular, we show how the point patterns produced by the intersection of threading dislocations with a film surface can be used to monitor and quantify the extent of dislocation clustering and array formation in GaN films. Such analyses enable us to discriminate between competing theories regarding dislocation origin in GaN films and to understand the interactions between defects better.

Thermal Etching of 6H-SiC and CVD Poly-Crystalline SiC: *Frezghi Kibrom*[1]; [1]University of Pretoria

The process by which SiC crystals decompose and both silicon and carbon atoms sublimate revealing defects at the surface by annealing is called Thermal etching. 6H-SiC and CVD Poly-crystalline SiC samples were annealed in computer-controlled Webb 77 vacuum at several temperatures ranging from 500ºC for 10hrs to 1800ºC for 10hrs. Images of Gemini Ultra 55 Zeiss SEM were taken. A significant difference was observed for the thermal etching behaviour of these two samples. Annealing of 6H-SiC at temperatures above 1400ºC exhibited step-bunching. The micro-pipes at this annealing temperature exhibited well-defined faceted openings related to the symmetry of the crystal. The SEM images of Necsa poly-crystalline SiC samples annealed from 1600ºC for 3hrs showed cavities and holes at defects on the surface. Whereas annealing of Necsa poly-crystalline-SiC at 1600°C for 3 hrs at cross-sectional investigation, severe thermal etching was observed at grain-boundaries and twins.

Tight Binding and LCAO Methods for Tin Oxide Deposited by Chemical Vapour Deposition and Spray Pyrolysis Techniques: *Nazia Kesri*[1]; [1]University of Sciences and Technology Houari Boumediene

This work outlines the fabrication by chemical vapour deposition (CVD) and by spray pyrolysis and the characterisation of transparent undoped tin oxide layers . The thin films were grown on glass substrates at atmospheric pressure. Deposition parameters, such as substrate temperature, time of deposition and oxygen flow (CVD) or nitrogen flow (spray) have been varied. Tin oxide crystallise in the rutile structure. X-ray diffraction study shows that the films were polycrystalline, with (110) preferential direction for deposition temperature at 400°C. For different deposition parameters, (101), (211) and (200) orientations become predominant. The optical band-edge absorption was studied experimentally by transmission and reflection spectra. The calculation of electronic structure of SnO2 was carried out using a semi-empirical tight binding method (LCAO). Nearest neighbour (tin oxygen) and second nearest neighbour parameters are included into s and p-states. The calculated and measured band gaps are compared to other theoretical and experimental values[1-4] .

Ultrasound Influence on the Recombination Centers in Silicon p-n-Structures: *Oleg Olikh*[1]; [1]Taras Shevchenko Kyiv National University

Recently the acoustic waves are used for controlled modification of the defect subsystem. This work is devoted to experimental investigation of the deep levels in *Cz*-Si *p-n*-structures under ultrasonic loading with the help of the method of the current-voltage characteristic differential coefficients. The longitudinal acoustic

waves with frequency 4-26 MHz and intensity up to 0.6 W/cm^2 were used. There levels with activation thermal energy 0.44, 0.40, 0.37, 0.48 and 0.46 eV were detected. It is suggested that these levels related to the E-centre, the bistable complex B_sO_{2i} and interstitial atoms captured on dislocation loops respectively. It is revealed that ultrasound induces the increase of the shallow levels contribution into carrier recombination and this process depends linearly on sound wave strain. The decrease of the defects activation energy under ultrasound action is observed too. The possibility of the acoustoinduced reversible changes of the B_sO_{2i} configuration is analyzed.

X-Ray Diffraction Imaging of Improved Bulk Grown CdZnTe (211) and its Comparison to Epitaxially Grown CdTe Buffer Layers on Si and Ge Substrates: *Justin Markunas*[1]; Tony Almeida[1]; Randolph Jacobs[1]; Joe Pellegrino[1]; Syed Qadri[2]; Nadeem Mahadik[2]; Jas Sanghera[2]; [1]US Army Night Vision Laboratory; [2]US Naval Research Laboratory

Large area, high quality (Hg,Cd)Te sensing layers for infrared imaging in the 8-12μm spectral region are typically grown on (Cd,Zn)Te substrates. Research efforts have focused on growing high quality bulk CdZnTe. Much of this bulk grown CdZnTe showed defects, small angle grain boundaries, high dislocation densities and other extended defects. Recent progress in bulk growth by the liquid encapsulation Czochralski method has produced substrates with a rocking curve full width half maximum under 20 arc seconds. Alternatively, epitaxial CdTe grown on Si or Ge has been used as a buffer layer for high-quality epitaxial HgCdTe growth. The best epitaxially grown CdTe with thicknesses in the 8-10μm range had a rocking curve full width at half maximum on the order of 70 arc seconds. In this paper, x-ray topographs will be presented of recent high-quality bulk grown CdZnTe, epitaxial CdTe buffer layers and previous bulk grown substrates for comparison.

X-Ray Diffraction Study of MBE-Grown CaF2-CdF2 Superlattices on Si(111): *Gleb Valkovsky*[1]; M. Baidakova[1]; S. Konnikov[1]; A. Krupin[1]; R. Kyutt[1]; N. Sokolov[1]; S. Suturin[1]; M. Yagovkina[1]; [1]Ioffe Physical-Technical Institute of the Russian Academy of Sciences

Structure of CaF2-CdF2 superlattices (SLs) grown by MBE on Si(111) with the period ranging from 1.5 to 20 nm has been studied by x-ray diffraction methods. High-resolution x-ray diffraction analysis has revealed, that a partial strain relaxation occured in the SLs with the period $t > 20$ nm. The SLs with $t < 20$ nm can be grown pseudomorfically, but x-ray diffraction analysis has demonstrated the presence of transition layers in these SLs. The layers in our case could be due to roughness of CaF2-CdF2 inner interfaces. The amount of interfacial roughness, its evolution, the degree of correlation has been obtained from a fit of small-angle x-ray scattering data. The results of our investigation have been provided a coherent picture with AFM data. A possible mechanism of inheritance of roughness has been considered.

Compound Photovoltaics

Tuesday AM Room: Glessner Auditorium
September 15, 2009 Location: Oglebay Resort & Conference Center

Session Chair: Michio Tajima, Institute of Space and Astronautical Science/JAXA

8:30 AM Invited

Solar Photovoltaics Research and Technology: The Revolution Begins...: *Lawrence L. Kazmerski*[1]; [1]National Renewable Energy Laboratory

The growing prospects of current and coming solar-photovoltaic (PV) technologies are envisioned, arguing this solar-electricity source is exactly at a tipping point in the complex worldwide energy outlook. The co-requirements for policy and technology investments are strongly stressed. The emphasis of this presentation is on research and technology advances (cell, materials, and module options. The contributions and technological pathways for now and near-term technologies (silicon, III-Vs, and thin films) and status and forecasts for next-generation PV (organics, nanotechnologies, non-conventional junction approaches) are evaluated. These are contrasted with looks back over the past 50-year history that this technology has been nurtured—demonstrating what we have already learned and cataloging some key contributions to our modern life. Recent advances in concentrators with efficiencies headed toward 50%, new directions for thin films (20% and beyond), and materials/device technology issues are discussed in terms of technology progress. Insights into technical and other investments needed to tip photovoltaics to its next level of contribution as a significant clean-energy partner in the world energy portfolio. The need for R&D accelerating those imminent (evolutionary) technologies balanced with work in mid-term (disruptive) approaches is highlighted. Moreover, technology progress and ownership for next-generation solar PV mandates a balanced investment in transformational research on longer-term (the revolution needs revolutionary approaches to sustain itself) technologies (quantum dots, multi-multijunctions, intermediate-band concepts, nanotubes, bio-inspired, thermophotonics, solar hydrogen. . .) having high-risk, but extremely high performance and cost returns for our next generations of energy consumers. Issues relating to manufacturing are explored—especially with the requirements for the next-generation technologies. This presentation provides insights into how this technology has developed—and where we can expect to be by this mid-21st century.

9:00 AM Invited

The Impact and Control of Defects in III-V/Si Heterostructures for Photovoltaics: *Steven Ringel*[1]; [1]Ohio State University

The desire to epitaxially integrate III-V heterostructures with silicon substrates for solar cell applications has been a driving force for advanced photovoltaics research for more than two decades. The rationale for this interest stems from the need to achieve a solar cell technology that simultaneously possesses very higher energy conversion efficiency, hence the application of III-V materials and III-V multijunction solar cell structures, but at a manageable cost, hence the interest in using Si substrates for creation of III-V/Si solar cell technology. The ability to integrate existing high performance III-V solar cell materials with existing high quality Si substrates places the research burden almost entirely on solutions that manage and mitigate crystalline defects that arise due to mismatches in various structural and chemical properties between epitaxial III-V materials and Si. This paper focuses on defect formation, characterization and control in two III-V/Si material systems, GaInP/GaAs/SixGe1-x/Si and GaAsyP1-y/Si, both of which are leading contenders for III-V/Si photovoltaic technologies. In both cases, the ability to simultaneously suppress and eliminate threading dislocations, antiphase domain boundaries, stacking faults and other defect formations is essential for successful solar cell technology since preservation of low minority carrier recombination rates and eliminating parasitic current leakage paths is required. However, important differences exist in these relatively parallel approaches, especially from the perspective of dominant defect modes and their sources as they relate to lattice mismatched interfaces and chemical dissimilarities at those interfaces. This presentation considers this in detail throughout the process of demonstrating direct correlations between various structural defects, electronic materials properties and devicecharacteristics for both III-V/Si systems.

9:30 AM

Application of CL/EBIC-SEM Techniques for Characterization of Multi-junction Solar Cells: *Serguei Maximenko*[1]; Corry Cress[1]; Jeffrey Warner[1]; Jaime Freitas, Jr.[1]; Scott Messenger[1]; Robert Walters[1]; [1]Naval Research Laboratory

Multijunction III-V semiconductors' based solar cells grown on Ge are the premier space photovoltaic technology due to the high efficiency and radiation tolerance. However, the drive for higher energy density and enhanced reliability continues to motivate research in novel III-V multijunction solar cell design. Presently characterization of these devices is still a challenge. In the present work, we report the results of the characterization of irradiated triple junction solar cells by Cathodoluminescence (CL) imaging/spectroscopy and Electron Beam Induced Current (EBIC). These techniques were applied to verify the influence of irradiation damage on the opto-electronic properties of each individual junction cell and correlate with their Quantum efficiency performance.

9:45 AM

Detection and Recognition of Defects in Triple-Junction Solar Cell by Electroluminescence Imaging: *Shanshan Chen*[1]; Tomoya Ogawa[2]; Shuping Li[1]; Junyong Kang[1]; [1]Engineering Research Center for Micro-Nano Optoelectronic Materials and Devices of State Education Ministry, Xiamen University; [2]Crystal Technology Laboratory

Multi-junction (MJ) solar cells have a great potential for achieving high conversion efficiencies of over 30% and are promising for space and terrestrial applications. The highest efficiency MJ solar cells available so far are based on III-V semiconductors that are epitaxied on a single crystalline Ge substrate. Characterization of these devices, however, is still challenging, especially the experimental access to information about individual subcells. Electroluminescence (EL) has been demonstrated to be a powerful tool providing resolved information about the electrical, optical, and material properties of solar cells if combing with other methods such as quantum efficiency measurement or photography. In this report, we introduce a method to derive defect information of each individual subcell in triple-junction solar cells by combining electroluminescence (EL) with photographic measurement.

10:00 AM Break

Defects in Silicon

Tuesday AM Room: Glessner Auditorium
September 15, 2009 Location: Oglebay Resort & Conference Center

Session Chair: Piotr Edelman, SemilabSDI

10:30 AM Invited

Imaging of Metal Precipitates in Silicon by Luminescence Spectroscopy and Synchrotron Techniques: *Martin Schubert*[1]; [1]Fraunhofer Institute for Solar Energy Systems ISE

Metallic impurities in silicon, precipitated or dissolved, frequently limit the conversion efficiency of solar cells. Impurities, commonly in interaction with crystallographic defects reduce the recombination lifetime of free carriers. Furthermore, shunts as well as reverse breakdown sites may be induced. Detection techniques for dissolved and precipitated transition metals in silicon by fast luminescence imaging and by luminescence spectroscopy with highest resolution are discussed. Band to band recombination as well as defect luminescence is considered. Results on the precipitate distribution in both, industrial multicrystalline silicon, and model systems of intentionally contaminated monocrystalline silicon with defined dislocation networks are presented. X-ray fluorescence spectroscopy measurements at the ESRF synchrotron complement the detection of precipitates.

11:00 AM

Photoluminescence Analysis of Iron Contamination Effect in Multicrystalline Silicon Wafers for Solar Cells: *Michio Tajima*[1]; Masatoshi Ikebe[1]; Yoshio Ohshita[2]; Atsushi Ogura[3]; [1]Institute of Space and Astronautical Science / JAXA; [2]Toyota Technological Institute; [3]Meiji University

We investigated the effect of iron contamination on the electronic properties of dislocation clusters and oxygen precipitates in multicrystalline silicon (mc-Si). Photoluminescence (PL) spectroscopy at 300K and 4.2K and monochromatic PL

intensity mapping at 300K were performed on mc-Si wafers before and after iron contamination. PL spectra consisted of the band-edge emission, the 0.78 eV emission associated with oxygen precipitates, and the dislocation-related D-lines. Intensity mapping of the band-edge emission revealed the dislocation clusters as dark lines, and the majority part appeared as bright lines in mapping of the 0.78 eV emission, suggesting that the majority part of the dislocation clusters act as preferential oxygen precipitation sites. The iron contamination increased the electrically active dislocation clusters. The electronic property of the dislocation clusters was changed as indicated by the spectral change of D-lines. In contrast, the oxygen precipitates along the dislocation clusters were not influenced by the iron contamination.

11:15 AM

Quantitative Photoelastic Characterization of Residual Strains in Grains of Multi-Crystalline Silicon: *Masayuki Fukuzawa*[1]; Masayoshi Yamada[1]; Rafiqul Islam[2]; Jun Chen[3]; Takashi Sekiguchi[3]; [1]Kyoto Institute of Technology; [2]Khulna University of Enginerring and Technology; [3]National Institute of Material Science

The residual strain and its variation in the multicrystalline Si wafers (mc-Si) for solar cell were quantitatively characterized by scanning infrared polariscope (SIRP). The phase retardation δ and the principal axes Ψ of strain-induced birefringence were measured at each point in grains. The crystallographic orientations of the grains were also characterized by electron-back-scatter-diffraction (EBSD) technique. With these data, the strain was calculated by considering the anisotropy of photoelastic coefficients. It was clarified that the residual strain was large at the grains with multi-twin boundaries and the vicinity of small-angle grain boundaries, which reached to the order of 10^{-4}, corresponding to 10 MPa in stress.

11:30 AM

Observation of Two-Dimensional Distribution of Lattice Inclination and Strain in Strained Si Wafers by Synchrotron X-Ray Topography: *Takayoshi Shimura*[1]; Tomoyuki Inoue[1]; Daisuke Shimokawa[1]; Takuji Hosoi[1]; Heiji Watanabe[1]; Atsushi Ogura[2]; Masataka Umeno[3]; [1]Osaka University; [2]Meiji University; [3]Fukui University of Technology

Strained Si technology has attracted substantial attention as a means of enhancing carrier mobility in MOSFETs and thereby extends the limits of device miniaturization and performance. One of the methods available for the fabrication of strained Si devices involves the use of strained Si wafers. However, the crystalline quality of the strained Si wafers fabricated to date remains poor compared to conventional SOI wafers. It is therefore important to evaluate the crystalline quality of the strained Si wafers in order to continue improving this technology. In this paper we show two-dimensional distributions of lattice inclination and strain in strained Si wafers obtained by synchrotron x-ray topography. We observed a series of x-ray topographs obtained by changing the incident angle and derived rocking curves at each pixel of CCD detector. Lattice inclination and strain distributions were estimated by comparing the rocking curves measured at different azimuth angles.

11:45 AM

Correlation between Oxygen Precipitation and Generation of Extended Defects in Czochralski Silicon: Investigation by Means of Scanning Infrared Microscopy: Yuheng Zeng[1]; *Deren Yang*[1]; Xiangyang Ma[1]; Jiahe Chen[1]; Duanlin Que[1]; [1]Zhejiang University

Oxygen precipitates and secondary defects in Czochralski silicon (CZ-Si) have received extensive and intensive investigations in the past decades. However, the critical size of oxygen precipitates for inducing secondary defects remains somewhat unclear. In this paper, size effect of oxygen precipitates on secondary defects in the CZ-Si specimens subjected to different isothermal annealing was investigated by scanning infrared microscopy (SIRM). It was found that secondary defects generated in the case that oxygen precipitates grew to a certain size, as it was believed that interstitial Si (I) atoms preferred to aggregate to oxygen precipitates larger than a certain size, which we denoted as the critical size to induce secondary defects. Upon generation of secondary defects, the critical size remains nearly unchanged in the extending annealing. However, the critical size would reduce with annealing at higher temperatures or with higher I-atom concentration. Finally, the reason for the above results was discussed.

12:00 PM

Characteristic Aspects of Low-Temperature Elastic Softening Due to Vacancies in Boron-Doped FZ Silicon Crystals: *Hiroshi Yamada-Kaneta*[1]; Hajime Watanabe[1]; Yuta Nagai[1]; Shotaro Baba[1]; Mitsuhiro Akatsu[1]; Yuichi Nemoto[1]; Terutaka Goto[1]; [1]Niigata University

We recently found that the vacancy causes the *elastic softening* at low temperatures whose magnitude gives the vacancy concentration. The softening of B-doped silicon was characterized by the following behaviors: (1) The softening suddenly starts at around 5 K in cooling the sample, and (2) the softening is weakened by the applied magnetic field to vanish at nearly 3 T, in contrast to the softening of the non-doped silicon. Here, we confirm that these characteristics in the softening is general for (and inherent to) the B-doped silicon crystals containing the positively charged vacancies. From various positions in an ingot of B-doped FZ silicon crystal grown by Sumco TechXIV Corporation, we cut out many samples for the ultrasonic measurements for the softening. For all the samples, the observed softenings exhibited the above-mentioned characteristics, although their magnitudes varied on the ingot position. The origin of this characteristic behavior will also be addressed.

12:15 PM

Optimization of Silicon Ingot Quality by the Numerical Prediction of Bulk Crystal Defects: Fabrice Loix[1]; *François Dupret*[2]; Arnaud de Potter[1]; Wu Liang[1]; Roman Rolinsky[1]; Nathalie Van den Bogaert[1]; [1]FEMAGSoft S.A.; [2]UCL

We will here focus on the prediction of Si ingot quality grown by Czochralski process and its optimization by means of numerical simulation. We present a fully time-dependent model devoted to predict the global heat transfer in a furnace, the solid-liquid interface shape, and the resulting distributions of point- and micro-defects as calculated from the Sinno-Dornberger (S-D) model together with an extension of the lumped model of Voronkov and Kulkarni. In addition to the classical point-defect evolution mechanisms, a new lumped model is developed to calculate the formation and growth of micro-defects in order to predict their densities and size distributions anywhere in the crystal. Another key issue in Czochraslki Si growth is to control the density of oxygen and any other species (including dopants and impurities) inside the crystal. Modeling issues will be here again detailed.

Organic Photovoltaics and OLEDs

Wednesday AM Room: Glessner Auditorium
September 16, 2009 Location: Oglebay Resort & Conference Center

Session Chair: Steven Ringel, Ohio State University

8:30 AM Invited
Lifetime Studies of Plexcore Ink Systems: Enabling Low–Cost Large–Area OPV Solar Power: Darin Laird[1]; *Christine McGuiness*[1]; [1]Plextronics

As the global demand for energy escalates, renewable energy resources such as solar power become viable commercial options provided solar power's levelized cost of efficiency (LCOE) or power out over the course of the lifetime of the device is competitive with current energy technologies. Printed solar cells based on organic photovoltaic (OPV) devices have the potential for dramatic cost savings over current solar technologies due to low cost manufacturing methods and thin, light-weight polymer-based composition. Although single-layer OPV devices are projected to have efficiency limitations of 10-12%, these systems have the potential for competitive lifetimes up to and greater than 15 years. Plextronics, Inc. is helping seed the renewable energy OPV market by developing the core polymers and ink systems for enabling the large-scale manufacture of printed OPV modules. We have demonstrated world-leading, National Renewable Energy Laboratory (NREL) certified OPV cell efficiency of 5.98% using our inks and process technology for glass substrates. The technology has been scaled up to larger area modules (15.2 cm × 15.2 cm module size), which was certified by NREL as having 2.05% total area efficiency (4.24% active area efficiency). Besides driving the efficiency towards commercially viable metrics, we have established a world-class OPV lifetime testing facility to evaluate OPV ink stability and the lifetimes of OPV devices. These testing facilities include the ability to correlate outdoor, rooftop testing conditions in multiple worldwide locations and acceleration tests, including extreme temperature, light intensity and humidity conditions, to project and improve the lifetime of OPV devices. Here, we will discuss methodology for standard lifetime testing which will lead to meaningful projections of the lifetime of OPV devices and modules based on Plextronics' PV ink systems.

9:00 AM Invited
Toward the Unified View of Nanostructure-Defects-Transport Relationships in Conducting Polymers: *Tomasz Kowalewski*[1]; [1]Carnegie Mellon University

One of the outstanding challenges in the field of organic semiconductors, in particular those of macromolecular nature, is the establishment of the relationship between their structure, defects and transport properties. One of the potential advantages of polymer semiconductors in comparison with low-molecular weight systems is the possibility to achieve particularly extensive charge delocalization (and thus fast transport pathways) along the conjugated polymer backbone. Owing to their superior transport properties, regioregular poly(alkylthiophenes) (-rrPATs) emerged as one of the most widely studied semiconducting polymers with potential applications in organic electronics. This talk will present an attempt to define the unified view of types of nanostructures and defects observed in semiconductor devices based on rr-P3ATs and their derivatives. Special emphasis will be placed on the impact of defects on performance of rr-P3AT based semiconductor devices such as field effect transistors and bulk heterojunction photovoltaic cells.

9:30 AM
Small Molecule/Metal Phthalocyanine Based Organic Photovoltaics: *Gary Kushto*[1]; [1]United States Naval Research Laboratory

Metal phthalocyanine complexes (MPcs) are known for nearly every metal in the periodic table; however, the complexes of copper and zinc are far and away the most commonly used p-type materials in small molecule organic photovoltaic (OPV) devices. It is clear that further investigation into the operational parameters of MPc-based OPVs is required. The present work will focus on OPVs fabricated using the phthalocyanine complexes of the groups 10 and 11 metals (Ni, Pd, Pt, Cu and Ag). A discussion of the groups 10 and 11 MPcs and how their molecular properties correlate with the observed trends in the OPV device characteristics will be presented.

9:45 AM
Deep-Level Optical Spectroscopy Investigation of Degradation in Alq_3-Based OLEDs: *Yoshitaka Nakano*[1]; [1]Chubu University

We have applied modified deep-level optical spectroscopy (DLOS) to degraded OLEDs based on Alq_3/α-NPD, and have investigated emissive interface states before and after the degradation. The OLED samples were degraded through the constant-current operation of 44.4 mA/cm^2. The final luminance decreased down to 30% of the initial value (1830 cd/m^2). After the degradation, the emissive interface trap is found to shift from ~1.77 to ~1.39 eV, being the same level as an Alq_3 single layer. Similarly, the peak position of near-band-edge transitions of Alq_3 also shifts to the lower photon energy side. These variations in band gap states are probably induced by the degradation and indicate that initial structural orientations peculiar to emissive interface are significantly transformed into bulk-like *relaxed* ones through the degradation. Thus, DLOS has been proven to be a powerful tool for understanding the intrinsic degradation in the OLEDs from the viewpoint of electronic states.

10:00 AM Break

Defects in SiC

Wednesday AM Room: Glessner Auditorium
September 16, 2009 Location: Oglebay Resort & Conference Center

Session Chair: Yoosuf Picard, US Naval Research Laboratory

10:30 AM Invited
Analysis of Defect Formation in 4H-SiC Epitaxial Growth by X-Ray Topography: *Hidekazu Tsuchida*[1]; Isaho Kamata[1]; Masahiro Nagano[1]; [1]Central Research Institute of Electric Power Industry

Extended defects in 4H-SiC epilayers have been surveyed by grazing incidence synchrotron reflection X-ray topography. The high-resolution topography defect contrast enables to distinguish each dislocation and stacking fault in the material. Generation, conversion and propagation of the extended defects, which are threading dislocations, basal plane dislocations, carrot defects, basal plane Frank-type defects and polytype inclusions, in 4H-SiC epitaxial growth are tracked by performing topography before and after the growth procedure. We also have made correlations between the detailed feature of topography contrast and the microscopic structure for the extended defects in a combination of X-ray topography, transmission electron microscopy and KOH defect selective etching analysis, and the formation mechanism of each type of defects is discussed.

11:00 AM
Comparative Study on the Dislocation Densities of 4H-SiC Substrates and Homoepitaxial Layers Using Defect Selective Etching and Synchrotron White Beam X-Ray Topography: *Birgit Kallinger*[1]; Sebastian Polster[1]; Patrick Berwian[1]; Jochen Friedrich[1]; Andreas Danilewsky[2]; Alexander Wehrhahn[3]; Arnd-Dietrich Weber[3]; [1]Fraunhofer IISB; [2]University of Freiburg; [3]SiCrystal AG

Dislocation types and their densities of 4H-SiC samples with different N doping concentrations have been investigated using Defect Selective Etching (DSE) in molten KOH and Synchrotron X-ray Topography (XRT). Comparison of etch patterns with x-ray topographs proofs that each dislocation is correlated to an etch pit and vice versa. For samples with N concentrations < 10^{18} cm^{-3} the size of hexagonal shaped etch pits reveals the type of threading dislocations. Contrary to literature, this dislocation identification by etch pit size is not true for higher N concentrations, e.g. for substrates. Furthermore, an additional etch pit type occurs for N concentrations in the order of 10^{17}-10^{18} cm^{-3} which corresponds to a certain type of dislocation. We will show that the doping concentration does influence the etching behaviour of 4H-SiC samples and demonstrate a more detailed model of the etching process.

11:15 AM
Observations of Screw Dislocation Driven Growth and Faceting during CVD Homoepitaxy on 4H-SiC on-Axis Mesa Arrays: *Philip Neudeck*[1]; Andrew Trunek[2]; J. Anthony Powell[3]; Yoosuf Picard[4]; Mark Twigg[4]; [1]NASA Glenn Research Center; [2]OAI; [3]Sest, Inc.; [4]US Naval Research Laboratory

Previous studies of (0001) homoepitaxial growth carried out on arrays of small-area mesas etched into on-axis 4H-SiC wafers indicate that spiral growth

emanating from at least one screw dislocation threading the mesa is necessary in order for a mesa to grow taller in the <0001> (c-axis vertical) direction while maintaining the 4H stacking sequence. However, even amongst mesas containing a screw dislocation spiral step source necessary for c-axis growth, we have observed significant differences in the height and faceting that evolve during prolonged homoepitaxial growths. This paper summarizes AFM, ECCI, SEM, and optical microscopy evidence that the observed large variation in growth behavior is related to the lateral position of a screw dislocation step source within the mesa. When the screw dislocation step source is located close enough to the edge/sidewall facet of a mesa, the c-axis growth rate and side facet slope are affected by the resulting interaction.

11:30 AM

Electro- and Photoluminescence Spectral Imaging of Extended Defects in 4H-SiC: *Joshua Caldwell*[1]; Robert Stahlbush[1]; Kendrick Liu[1]; Karl Hobart[1]; Orest Glembocki[1]; [1]Naval Research Laboratory

Understanding luminescence spectra from extended defects in semiconductor materials is required if their impact on the electronic or optoelectronic properties is to be understood. Typical luminescence spectroscopy collects light from too large of an area to differentiate the spectrum from individual extended defects. This lack of spatial information can lead to incorrect assignments of luminescence bands and therefore to a misinterpretation of the nature and mechanism of defects and their nucleation. We report on the collection and analysis of real-color and spectrally-selective monochromatic electro and photoluminescence imaging. Such imaging enables the simultaneious collection of both structural and spectral properties from extended defects. The measurements reported here were performed on 4H-SiC pin diodes and epitaxial layers as a function of injection level and length of injection. These efforts enabled the assignment of an emission centered at 510nm to carbon-core partial dislocations, in contrast to the previous assignment to B-related point defects.

11:45 AM

Electrical and Optical Properties of Stacking Faults in 4H-SiC Homoepitaxial Layers: *Bin Chen*[1]; Jun Chen[1]; Takashi Sekiguchi[1]; Takasumi Ohyanagi[2]; Hirofumi Matsuhata[2]; Akimasa Kinoshita[2]; Hajime Okumura[2]; [1]National Institute for Materials Science; [2]National Institute of Advanced Industrial Science and Technology

4H-SiC is a wide band-gap semiconductor suited for applications in high-power, high-temperature and high-frequency electronics. However, the killer defects for the breakdown or degradation phenomenon in 4H-SiC devices have not been fully clarified yet. According to the recent studies, one harmful defect is the stacking fault (SF). We have observed the recombination-enhanced SF formation under the electron beam irradiation. The electrical and optical properties of SF were characterized by using electron-beam-induced current (EBIC) and cathodoluminescence techniques. We found that the SFs are bright in EBIC images at RT. We propose a quantum well model of SF to explain this peculiar EBIC contrast. The formation mechanism of SF and the effect of impurities on SF generation are also discussed in this presentation.

12:00 PM

Study on Nucleation Mechanism of Polytype Transformation in 6H and 15R SiC Crystals: *Yu Zhang*[1]; Hui Chen[1]; Michael Dudley[1]; James Edgar[2]; Krzysztof Grasza[3]; Emil. Tymicki[3]; Yimei Zhu[4]; [1]Stony Brook University; [2]Kansas State University; [3]Institute of Electronic Materials Technology; [4]Brookhaven National Laboratory

Nucleation mechanism of polytype transformation in 6H and 15R SiC was studied using Synchrotron White Beam X-Ray Topography, monochromatic X-Ray topography and high resolution transmission electron microscopy. According to the model, inhomogeneous densities of screw dislocations replicated from the seed lead to uneven growth rates resulting in a quasi-vicinal growth surface. Subsequent interference between advancing vicinal steps and screw dislocation spiral steps lead to complex step overgrowth processes which can suppress all or part of the 15R 1c screw dislocation Burgers Vector(BV) through the creation of Frank faults and Frank partial dislocations. Combined with stacking shifts induced by the passage of basal plane partial dislocations it is shown that suppression of 9/15 of the 15R 1c dislocation BV can leave behind a residual BV corresponding to a 1c dislocation in 6H-SiC. This residual dislocation then acts as a nucleus for reproduction of the 6H SiC structure.

12:15 PM

Phonon Assisted Tunneling in Z1/Z2 Defect in 4H-SiC: *Andrew Evwaraye*[1]; [1]University of Dayton

The application of strong static electric fields to semiconductors containing deep impurity levels leads to enhanced emission rates from these centers. These increased emission rates are normally explained by invoking one of three mechanisms—the Poole-Frankel effect, phonon assisted tunneling and direct tunneling. The Poole-Frankel effect occurs only for charged impurities and can be observed for relatively small electric fields (104 V/cm). Phonon assisted tunneling and direct tunneling occur for defects in any charge state. Bulk n-type 4H-SiC wafers with net doping concentration of 2.5 x 1017 cm-3 were irradiated with 1 MeV electrons at different doses. The thermal emission rates from Z1/Z2 defect levels were studied at different electric fields in the junction using double-correlation deep level transient spectroscopy (DDLTS). Analysis of the data unambiguously shows that the observed electric field enhancement of the emission rates is due to phonon assisted tunneling.

Defects in Nitrides

Wednesday PM Room: Glessner Auditorium
September 16, 2009 Location: Oglebay Resort & Conference Center

Session Chair: Mark Twigg, Naval Research Laboratory

1:30 PM Invited

Cathodoluminescence Characterization of Free-Standing GaN Wafers: *Takashi Sekiguchi*[1]; Woong Lee[1]; Benjamin Dierre[1]; Masaaki Yokoyama[2]; Hyun Jae Lee[3]; Jiho Chang[3]; Takafumi Yao[3]; [1]National Institute for Materials Science; [2]Horiba Ltd.; [3]Tohoku University

Free standing GaN wafers are expected as the substrates for advanced blue lasers or LEDs due to strain-free nature. However, there still exist several types of defects and/or non-uniformities in these wafers. We have applied cathodoluminescence (CL) to characterize free-standing (0001) GaN wafers grown by HVPE and elucidated the origin of imperfections. In monochromatic CL image of band edge emission, we found bright patterns of hexagonal or round shape around 50 micron in size. These bright areas correspond to the concave area of as-grown ingots. This infers that the difference of the growth facet is the origin of these imperfections. Most of the patterns have dark cores and six-folded diagonals. The careful analysis of CL pattern suggests us the formation mechanism of concave facets and the way to remove them.

2:00 PM

Evidence for Dislocation Movement by Climb in GaN Films: *Michelle Moram*[1]; Menno Kappers[1]; Colin Humphreys[1]; [1]University of Cambridge

The bulk equilibrium vacancy concentrations and self-diffusion constants in GaN are expected to be low, even at elevated growth temperatures. As a result, threading dislocation climb in GaN was thought to be unlikely. However, we consistently observe a decrease in the threading dislocation density and an increase in the degree of dislocation array formation after annealing GaN films, as revealed by atomic force microscopy and by cathodoluminescence studies in the scanning electron microscope. These data are consistent with thermally activated dislocation climb. We have further studied the effect of growth conditions on dislocation climb by altering the V-III ratio during film growth, leading to the incorporation of high, non-equilibrium concentrations of Ga and N vacancies. The effects of film growth and annealing conditions on the extent of dislocation climb will be presented, along with evidence relating to possible climb mechanisms in GaN.

2:15 PM

Stacking Mismatch Boundaries in 2H-AlN Grown on 6H-SiC (0001) Vicinal Substrates with 3-Bilayer-Height Steps by Molecular-Beam Epitaxy: *Hironori Okumura*[1]; Masahiro Horita[1]; Tsunenobu Kimoto[1]; Jun Suda[1]; [1]Kyoto University

SiC is one of the most suitable substrates for heteroepitaxial growth of AlN due to its small lattice mismatch to AlN (1%). However, AlN and SiC have the different polytypes; wurzite (2H) structure (ABAB…) and 6H structure (ABCACBABCACB…), respectively. It is important to understand formation

mechanism of extended defects in AlN layers due to the polytype difference. We grew 2H-AlN layers on 6H-SiC (0001) vicinal substrates with 3-bilayer-height steps by MBE. Planar defects threading through the AlN layer were observed at the step edges of the SiC substrate by TEM. The planar defects formed boundaries. We concluded that the planar defects were stacking mismatch boundaries (SMBs) owing to the difference in stacking sequence of 2H and 6H structure. The SMBs were not observed at some step edges of the SiC substrate, suggesting control of the SiC surface is a key to eliminate SMBs.

2:30 PM

Stress Relaxation in GaN Epilayers Grown by MOCVD with Indium Surfactant: *Dongjin Won*[1]; Joan Redwing[1]; [1]Pennsylvania State University

Indium has been proposed to act as a surfactant during the growth of GaN thin films by MOCVD resulting in a change in the surface energetics, film morphology and strain. In this study, the effect of indium on the growth of GaN films on SiC substrates at 950°C was investigated using a combination of in-situ wafer curvature measurements and post-growth characterization techniques. As the molar flow rate of trimethylindium (TMIn) was varied from 0 to 4.5 μmol/min, the mean compressive stress of the GaN films at growth temperature decreased from -0.60 to -0.30 GPa which corresponded with an increase in the size and density of inverted hexagonal defects (V-pits). The driving force for V-pit formation was calculated and was found to provide a satisfactory explanation for the increase of V-pits with increasing indium concentration and the measured stress relaxation.

2:45 PM

K2S2O8-KOH Etching System for Revealing Defects and Pattern Etching of GaN: *Jan Weyher*[1]; Dennis van Dorp[2]; John Kelly[2]; Boleslaw Lucznik[1]; Frans Tichelaar[3]; [1]Institute of High Pressure Physics; [2]University of Utrecht; [3]National Centre for HREM

In this presentation we will report the results of open-circuit photo-etching experiments performed in KSO-KOH etching solutions. The mechanism of surface reactions will be briefly described and optimal etching composition for both revealing defects and for pattern etching will be presented. Numerous examples of defects which can be revealed in GaN and SiC using this etching system will be shown. The KSO-KOH etching system will be critically compared to the classical PEC etching in KOH solutions and to orthodox etching in molten salts. Calibration of etching by TEM confirms association of etch patterns with dislocations in GaN and will be demonstrated.

3:00 PM

Characterization of Tensile Stress Induced by Inclined Threading Dislocations in Si-Doped $Al_xGa_{1-x}N$: *Ian Manning*[1]; Xiaojun Weng[2]; Jeremy Acord[3]; Mark Fanton[3]; David Snyder[3]; Joan Redwing[4]; [1]Pennsylvania State University; [2]Materials Research Institute; [3]Pennsylvania State Electro-Optics Center; [4]Pennsylvania State University/Materials Research Institute

Si-doped and nominally undoped $Al_xGa_{1-x}N$ films with $0 < x < 0.62$ were grown on SiC substrates by MOCVD. The films were characterized using *in situ* wafer curvature measurements and TEM. The evolution of biaxial stress was correlated with edge-type threading dislocation inclination. In undoped $Al_xGa_{1-x}N$ films grown on AlN buffer layers, lattice mismatch induces an initial compressive biaxial stress, which relaxes as film thickness increases. A marked increase in the rate of relaxation, followed by a transition to tensile biaxial stress was observed upon introduction of Si at Si concentrations greater than 3.2×10^{18} cm^{-3} for $x = 0.62$, and similarly for $x = 0.4$. The rate of tensile stress generation was found to increase with increasing Si concentration. The inclined dislocation density was found to decrease with doped film thickness, allowing refinement of an earlier stress relaxation model in which dislocation density was assumed to be constant.

3:15 PM

Investigation of Heterostructures Based on AlInGaN by Local Methods: *Yana Domracheva*[1]; Tatiana Popova[1]; Ekaterina Flegontova[1]; Maria Zamorynskaya[1]; [1]Ioffe Physical-Technical Institute of the Russian Academy of Sciences

Nitrides AlInGaN are promising materials for optoelectronic device applications. However wide range of typical defect phenomena like InGaN phase separation, In segregation, high dislocations density determine luminescent properties of structures based on AlInGaN solid solutions. Such extremely high level of inhomogeneity of this material has generated a need in new experimental techniques. In this work a new approach for AlInGaN investigation was worked up. This approach was based on combined use of electron probe microanalysis, local cathodoluminescence and mathematical simulation. This technique allows studying peculiarities of the content distribution and luminescent properties in the growth direction in a nondestructive way. In this work it was shown that this combined technique allows determining extent of phase separation, radiation transport peculiarities induced by electron traps and a number of other important parameters. The work was performed at the JRC "Material science and characterization in advanced technology" and supported by ADPP (project 988).

3:30 PM Break

Defects in Devices

Wednesday PM, September 16, 2009
Room: Glessner Auditorium
Location: Oglebay Resort & Conference Center

Session Chair: Jean-Pierre Landesman, Institut des Matériaux Jean-Rouxel, CNRS and Nantes University

4:00 PM Invited

Reliability Investigations on High-Power, High-Brightness Semiconductor Lasers: *Ute Zeimer*[1]; Bernd Sumpf[1]; Karl Häusler[1]; Götz Erbert[1]; [1]Ferdinand-Braun-Institut für Höchstfrequenztechnik

High-brightness red emitting diode lasers are key devices for laser display technology. Due to the lower efficiency and higher temperature sensitivity compared to NIR diode lasers it is challenging to get the necessary requirements for reliability. Both broad area and tapered lasers emitting at 650 nm based on InGaP quantum wells embedded in AlInGaP waveguide layers are developed. These devices deliver output powers in the Watt-range. Device properties and a study of the aging behavior over several 1000h will be presented. Analysis of failed devices is carried out by optical microscopy and electro-luminescence imaging from the front facets as well as by near field measurements and wavelength resolved cathodoluminescence. The influence of mounting induced stress and operation temperature on the reliability will be discussed.

4:30 PM

Defect Imaging in Laser Diodes by Mapping Their Infrared Emission: *Jens Tomm*[1]; [1]Max-Born-Institut

We report on the use of infrared emission in the 1-2 μm spectral range from diode lasers that have their primary emission in the visible or near-infrared spectral range up to 980 nm. We address the nature of this extra infrared emission from various types of GaAs-based devices. We find three additional low-energy lines of spontaneous emission assigned to bandtail-related luminescence from the gain region, and interband and deep-level-related luminescences from the GaAs substrate. With this knowledge we mapped a number of high-power diode laser arrays with respect to this type defect-related emission. Fur this purpose a thermocamera has been used while limiting the detection range to the near infrared. Both brighter and poorer emitting areas are indicative for different mechanisms that affect the reliability of the devices. The mechanisms are discussed based on the analysis of samples from different batches.

4:45 PM

Investigation of Thermal Effects in Quantum Cascade Lasers: *Kamil Pierscinski*[1]; Dorota Pierscinska[1]; Kamil Kosiel[1]; Anna Szerling[1]; Maciej Bugajski[1]; [1]Institute of Electron Technology

The quantum cascade lasers (QCLs) are the most advanced class of semiconductor sources of midinfrared radiation. QCLs suffer, however, from large current densities, resulting in high active region temperatures, which make room temperature continuous wave (CW) operation still difficult to achieve. Progress in thermal management and better understanding of thermal effects are needed for further development of quantum cascade lasers. In this paper we use spatially resolved thermoreflectance (SRTR) to measure temperature distribution over the facet of pulsed operated quantum cascade lasers. The presented method gives an insight into distribution and relative importance of heat sources within the laser. It also allows for determination of thermal resistance of the laser and to evaluate the in-plane $k_{parallel}$ and the cross-plane k_{perp} thermal conductivities of the active region which enables validation of a two-dimensional model for the anisotropic heat diffusion in QCLs.

5:00 PM

Investigation of Leakage Current of AlGaN/GaN HEMTs under Pinch-off Condition by Electroluminescence Microscopy: *Martina Baeumler*[1]; Michael Dammann[1]; Frank Gütle[1]; Helmer Konstanzer[1]; Wilfried Pletschen[1]; Rüdiger Quay[1]; Patrick Waltereit[1]; Michael Mikulla[1]; Oliver Ambacher[1]; Franck Bourgeois[2]; Reza Behtash[2]; Klaus Riepe[2]; Paul J. van der Wel[3]; Jos Klappe[3]; Thomas Rödle[3]; [1]Fraunhofer Institut für Angewandte Festkörperphysik; [2]United Monolithic Semiconductors; [3]NXP Semiconductors

Reduction of leakage currents under pinch-off conditions is necessary to improve the high voltage and long term stability of AlGaN/GaN HEMTs. We will present results from on-wafer electroluminescence (EL) microscopy on devices with leakage currents (Ileak) varying over four orders of magnitude. The EL images reveal a small band of enhanced EL along the drain side of the gate finger. We will demonstrate that in the off-state region the integrated EL intensity is proportional to Ileak independent of gate width for the devices under study. Plotting EL intensity as a function of gate voltage supports that below threshold the EL intensity follows the Ileak(UG)-dependence. The EL(UG) dependencies for positions of high and low EL intensity allow to identify areas of enhanced leakage currents for FIB cross-sections. Results after electrical stress will be discussed based on the question whether areas of enhanced leakage current have an impact on the degradation phenomena.

5:15 PM

Defect Formation in Electrically Degraded GaN High Electron Mobility Transistors: *Lingjia Li*[1]; Marek Skowronski[1]; [1]Carnegie Mellon University

In spite of their extraordinary performance, the wide spread use of AlGaN/GaN high electron mobility transistors is delayed by reliability issues. It has been found that device characteristics, such as gate current, drain current, and output power, degrade after high electric field DC stress. Electroluminescence images suggest non-uniform degradation along the gate with the formation of radiative recombination centers. Cross-sectional transmission electron microscopy performed at degradation sites revealed the formation of a pit-shaped defect at the drain-side edge of the gate during stress, accompanied by a crack-like defect extending from the bottom of the pit into the AlGaN/GaN epilayers. This observation is consistent with a defect formation mechanism associated with excessive inverse piezoelectric stress. These defects degrade device performance by trapping electrons and assisting electron tunneling between gate and channel, resulting in reduction of the sheet carrier concentration of the channel and lowering the Schottky barrier height of the gate.

5:30 PM

Detection of Device-Process Induced Extended Defects in 4H-SiC: *Masahiro Nagano*[1]; Hidekazu Tsuchida[1]; Takuma Suzuki[2]; Tetsuo Hatakeyama[2]; Junji Senzaki[3]; Kenji Fukuda[3]; [1]CRIEPI; [2]R&D Association for FED; [3]AIST

The detection of device-process induced extended defects in 4H-SiC during the ion-implantation/activation-anneal process was investigated by comparing synchrotron reflection X-ray topography images taken before and after the process. Aluminum, nitrogen and phosphorus ions were implanted and the annealing process was performed at 1670ºC. We have succeeded in detecting the formation of extended defects induced by the process, the formation modes of the extended defects are classified into (i) the generation of Shockley-type stacking faults near the surface of the epilayers, (ii) the generation of the BPD half-loops with interfacial dislocations near the epilayer/substrate interface, (iii) the migration of the preexisting BPDs with generation of dislocations near the implanted-layer/epiplayer interface or (iv) near the epilayer/substrate interface.

5:45 PM

Strain Mapping and Its Effect on Electrical Properties in Hetero-Structured AlGaN/GaN Devices: *Nadeemullah Mahadik*[1]; Syed Qadri[2]; Mulpuri Rao[1]; [1]George Mason University; [2]Naval Research Laboratory

Point-wise high resolution x-ray measurements were performed on AlGaN/GaN wafer to study the effect of localized strain on the transport measurements across the wafer. A whole wafer strain map of the AlGaN/GaN HEMT wafer showed a one-to-one correspondence with the variation in electrical resistivity. The in-plane strain variation is in the range of 2.295×10^{-4} – 3.539×10^{-4} resulting in a sheet resistance variation of 345 - 411 Ω/sq. Additionally, in-situ x-ray diffraction measurements, performed on AlGaN/GaN device structures under variable bias conditions, showed tensile strain for forward bias conditions, and compressive strain for reverse bias. Since the AlGaN/GaN interface has a high degree of piezoelectric polarization, these measurements were correlated with a variation of piezoelectric charges at the interface. A linear variation in the strain was observed with the bias voltage, which results in a change in the piezoelectric charge at the AlGaN/GaN interface with bias.

X-Ray Topography

Thursday AM Room: Glessner Auditorium
September 17, 2009 Location: Oglebay Resort & Conference Center

Session Chair: Hidekazu Tsuchida, Central Research Institute of Electric Power Industry

8:30 AM Invited
Developing Bright Field Synchrotron Imaging Techniques with Ultrahigh Spatial and Strain Sensitivity: *Xianrong Huang*[1]; [1]Brookhaven National Laboratory

Synchrotron X-ray topography is a fast and powerful technique for nondestructive characterization of bulk and epitaxial thin crystals, but conventionally it had various limitations, such as limited spatial or angular resolutions, thin probing depths. In this presentation, we will introduce a number of novel imaging techniques under development at NSLS and APS, including: 1) Bormann enhanced transmission imaging with penetration depth up to centimeters for ~9 KeV photons and <1 microradian lattice distortion sensitivity; 2) General bright-field imaging with no geometrical and diffraction distortions in mapping defects; and 3) Combination of nearly back-diffraction imaging and bright-field mapping, which can completely separate lattice misorientations and d-spacing changes and may map lattice constant variations with precisions up to the 10^-8 level or higher. We hope that our presentation will also encourage related users to propose a dedicated high-resolution diffraction/imaging beamline at the coming NSLS-II for wide applications of these new imaging techniques.

9:00 AM
Threading Screw Dislocations in 4H-SiC Wafer Observed by Weak-Beam Method in the Bragg-Case X-Ray Topography: *Hirotaka Yamaguchi*[1]; Hirofumi Matsuhata[1]; [1]National Institute of Advanced Industrial Science and Technology

Dislocations in 4H-SiC have been observed by X-ray topography in the Bragg-case (reflection) geometry by means of weak-beam technique. Using X-ray beam with an angular divergence of 0.18 arcsec collimated by an asymmetric Si 331 reflection, nearly-intrinsic rocking curve of SiC 0008 reflection was obtained. High-resolution contrast of threading-screw dislocations by kinematical diffraction was observed at a diffraction condition deviated from the rocking-curve peak by 5 arcsec. Threading screw dislocations running inside the wafer were projected on the topograph. In addition, sense of each screw dislocation was determined directly from the weak-beam image in consideration of lattice displacement around the dislocation. This technique is equivalent to the weak-beam dark-field image in electron diffraction, and it is shown that the weak-beam image in the Bragg-case X-ray topography enables cross-sectional observations from the surface without destruction.

9:15 AM
Defect-Related White-Light-Emissions of ZnO from $Mg_xZn_{1-x}O$/ZnO/SiO_x Heterostructures on Si: *Peiliang Chen*[1]; Xiangyang Ma[1]; Yuanyuan Zhang[1]; Dongsheng Li[1]; Deren Yang[1]; [1]Zhejiang University

In recent years research enthusiasm on ZnO has been greatly spurred due to the fact that ZnO is a wide-band-gap semiconductor with a direct band gap of ~ 3.37 eV at room temperature (RT) and a considerably large exciton binding energy of ~ 60 meV. It has been demonstrated that a variety of defects exist in undoped ZnO films, leading to efficient white-light-emissions. However, the previous reports on white-light electroluminescence (EL) of ZnO films are rare. Herein, we report the $Mg_xZn_{1-x}O$ (x<1)/ZnO/SiO_x (x<2) heterostructures on Si that can emit white light at RT. The detailed mechanisms of carrier transport and EL will be explained in the text.

9:30 AM
Stress Mapping Analysis by Ray Tracing (SMART): A New Technique for Residual Strain/Stress Measurement of Single Crystal Material Using Synchrotron White Beam: *Vishwanath Sarkar*[1]; Balaji Raghothamachar[1]; Shayan Byrappa[1]; Michael Dudley[1]; [1]SUNY at Stony Brook

Synchrotron X-ray topography is a well established characterization tool for analyzing defect structures and strain in single crystal materials. We have further extended this method to quantitatively measure the residual strain and stress in any single crystal. This is achieved by the modified technique of synchrotron X-ray topography, where a grid made out of X-ray absorbing material, placed in the path of incident or diffracted beam. By applying the principal of ray tracing to the recorded topographs all the six components of strain and stress tensor has been calculated and mapped over the entire area of the crystal. This novel non-destructive method of stress measurement can prove to be an invaluable tool for both single crystal manufacturers and users. Different geometries for obtaining reticulographs have been explored and discussed.

9:45 AM
Structural Characterization of Doped GaSb Single Crystals by X-Ray Topography: *Marcelo Honnicke*[1]; Irineu Mazzaro[2]; Juliana Manica[2]; Eraldo Benine[2]; E. M. da Costa[3]; B. A. Dedavid[3]; Cesar Cusatis[2]; Xianrong Huang[1]; [1]Brookhaven National Laboratory; [2]UFPR; [3]PUC-RS

GaSb single crystals with different dopants (Al, Cd and Te), grown by the Czochralski method, were characterized with x-ray topography and high angular resolution x-ray diffraction. Lang topography show dislocations parallel and perpendicular to the crystal surface. Double crystal x-ray topography show dislocations and vertical stripes on the GaSb (333) topography, which can be associated with circular growth bands. Rocking curve measurements were also acquired and compared with results predicted by the dynamical theory of x-ray diffraction. These measurements show that these GaSb single crystals have a variation in the lattice parameter better than 1E-5. This means that they can be used as electronic devices (x-ray detectors, for example) as well as x-ray monochromators.

10:00 AM Break

Defects in Materials

Thursday AM Room: Glessner Auditorium
September 17, 2009 Location: Oglebay Resort & Conference Center

Session Chair: Jens Tomm, Max-Born-Institut

10:30 AM
Synchrotron X-Ray Topography Study of Structural Defects and Strain in Epitaxial Structures of Yb- and Tm- Doped Potassium Rare Earth Double Tungstates and Their Influence on Laser Performance: Joan Carvajal[1]; *Balaji Raghothamachar*[2]; M Pujol[1]; X Mateos[1]; Michael Dudley[2]; Magdalena Aguiló[1]; Francesc Díaz[1]; [1]Universitat Rovira i Virgili; [2]Stony Brook University

Monoclinic potassium rare earth double tungstates, ($KRE(WO_4)_2$, RE = Y, Lu; KREW) are well suited as hosts for active lanthanide ion (Ln^{3+}) dopants for diode-pumped solid state lasers, with particular interest in thin disk laser configurations when they are grown as thin films. Thin active layers are obtained by growing epitaxial structures of highly doped KREW by the LPE method on undoped KREW substrates sliced from TSSG-grown boules. Using synchrotron white beam X-ray topography (SWBXT), we have imaged defects and strain in bulk substrates of different rare earth tungstates as well as within Yb^{3+} and Tm^{3+} doped epitaxies grown on them. Surface preparation and defect distributions in the substrates are correlated with the quality of overgrown epitaxies. The effect of doping levels and the growth conditions on the quality and thickness of the epitaxies is analyzed and compared with lasing efficiency to optimize laser emission for future thin-disk laser configurations.

10:45 AM
Importance of the Surface for the Luminescence Stability of ZnO: *Benjamin Dierre*[1]; Xiaoli Yuan[1]; Nicola Armani[2]; Filippo Fabbri[2]; Giancarlo Salviati[2]; Kazuyuki Ueda[3]; Takashi Sekiguchi[1]; [1]National Institute for Materials Science (NIMS); [2]IMEM-CNR Institute; [3]Toyota Technological Institute

Electron beam irradiation effects on the luminescence of ZnO crystal is a complicated problem. Indeed, a degradation of the ultraviolet luminescence usually occurs during cathodoluminescence (CL) measurements, but the degradation mechanisms have not been clarified yet. The evolution of the CL intensity strongly depends on the surface termination and the surface/volume ratio, which suggests that the surface plays a key role. To understand the role of the surface, we have treated the specimen by exposing atomic hydrogen and soaking on dilute HCl solution. The time-of-flight electron-stimulated desorption

(TOF-ESD) measurements were performed to clarify the H^+ and O^+ ions desorption. We find that the desorption of adsorbed hydroxyl and H originated from H-passivated defects is the key to explain the luminescence evolutions. We suggest that the control of the surface by coating is one way to improve the lifetime of optoelectronic devices.

11:00 AM

Far-Field Imaging of Nanoscale Dislocation Pits by Forescatter Electron Detection for Investigating 4H-SiC Defect Behavior: *Yoosuf Picard*[1]; Robert Stahlbush[1]; Brenda VanMil[1]; Serguei Maximenko[1]; Rachel Myers-Ward[1]; Jaime Freitas[1]; D. Gaskill[1]; Charles Eddy[1]; Mark Twigg[1]; [1]Naval Research Laboratory

Dislocations pose many problems for SiC-based devices. The ability to rapidly determine the position and identity of various dislocations in SiC is critical for converting, eliminating, or further characterizing them. Surface penetrating dislocations often produce characteristic shaped pits sub-micron in size and less than 100 nm deep. Forescatter electron detection (FED) is a simple strategy for enhancing topographic contrast in a scanning electron microscope sufficient to image and resolve these nanoscale pits. The FED approach is a straightforward, far-field imaging technique combining high angle tilting of the sample with appropriate diode detector positioning for recording low takeoff-angle electrons. The FED approach is coordinated with ultraviolet photoluminescence (UV-PL) to investigate the conversion behavior of BPDs to threading edge dislocations in 4H-SiC. Carrier diffusion lengths measured by the electron beam induced current (EBIC) technique are correlated to specific screw and edge dislocations delineated by the FED approach.

11:15 AM

Study of Metal Contamination in CMOS Image Sensors by Dark Current and Deep Level Transient Spectroscopies: *Florian Domengie*[1]; Jorge Luis Regolini[2]; Daniel Bauza[3]; [1]STMicroelectronics/IMEP-LAHC; [2]STMicroelectronics; [3]IMEP-LAHC

CMOS Image Sensors (CIS's) are receiving much attention for large volume electronic applications such as mobile phones, digital cameras, webcams, and automotive. CIS's pixel scalability is reducing pixel size down towards 1.0 µm. A serious challenge is to introduce improvements in crucial parameters such as the dark current per pixel which is affected by defects incorporated during the whole process. In a manufacturing line, the process yield loss due to accidental metallic contamination is hard to assess and solve. In the present article we study the detection and characterization of gold and tungsten metallic contamination in CIS's using Dark Current and Deep Level Transient Spectroscopies. Pixels are used to probe metal defects and observe electrical effects of individual atoms. Deep levels responsible for dark current are identified and their concentrations are calculated. Sensitivities of DCS and DLTS are evaluated to improve the defects detection capabilities available in production.

11:30 AM

Cathodoluminescence Study of InP Photonic Structures Fabricated by Dry Etching: Romain Chanson[1]; *Juan Jimenez*[1]; Frédéric Pommereau[2]; Jean-Pierre Landesman[3]; Ahmed Rhallabi[3]; [1]University Valladolid; [2]Alcatel-Thales III-V Laboratory; [3]Institut des Matériaux Jean-Rouxel, CNRS and Nantes University

InP-based photonic structures fabricated by dry etching, standard reactive ion etching with CH4/H2, or high density – inductively coupled plasma etching with SiCl4, were studied by spectrally resolved cathodoluminescence. Rectangular waveguides (different widths and dielectric masks), were fabricated in bulk InP. We observed the formation of defects inside and around the waveguides. These defects are non radiative recombination centers, and also induce residual stresses. Defect and stress distributions were imaged by CL spectrum imaging. The stresses were compressive inside the waveguides and were associated with the defects generated at the interface between the InP and the dielectric mask. The influence of the dielectric mask and the geometry (aspect ratio) of the waveguides was studied, showing a clear relation between the stress and defect distribution. The results are analyzed in terms of the defect generation revealed by the CL images and the potential heating of the structures during the etching process.

11:45 AM

Ion-Implantation Control of Ferromagnetism in (Ga,Mn)As Epitaxial Layers: O. Yastrubchak[1]; J. Domagala[2]; J. Sadowski[2]; M. Kulik[1]; J. Zuk[1]; A. Toth[3]; R. Szymczak[2]; *Tadeusz Wosinski*[2]; [1]UMCS, Institute of Physics; [2]Institute of Physics, Polish Academy of Sciences; [3]Research Institute for Technical Physics and Materials Science, Hungarian Academy of Sciences

Epitaxial layers of (Ga,Mn)As ferromagnetic semiconductor have been subjected to low-energy low-dose ion implantation by applying both the chemically active oxygen ions and inactive ions of neon noble gas. A number of complementary characterization techniques have been used with the aim to study an effect of ion implantation on the layer properties. Investigation of their electrical and magnetic properties revealed that the implantation with either O or Ne ions completely suppressed both the conductivity and ferromagnetism in the layers. On the other hand, Raman spectroscopy measurements evidenced that O ion implantation influenced optical properties of the layers noticeably stronger than Ne ion implantation. Moreover, structural modifications of the layers caused by ion implantation were investigated using high-resolution X-ray diffraction technique. A mechanism responsible for ion-implantation induced suppression of ferromagnetism in (Ga,Mn)As layers, which could be applied as a method for tailoring nanostructures in the layers, is discussed.

12:00 PM

Study of Multilayer Semiconductor Structures by Local Methods: *Maria Zamorynskaya*[1]; Yana Domracheva[1]; Tatiana Popova[1]; Alexey Shakhmin[1]; Denis Shustov[1]; Alexander Trofimov[1]; Samuil Konnikov[1]; [1]Ioffe Institute

In this paper we use complex of non-destructive local methods for characterization of multilayer semiconductor structures. Our latest investigation shows the possibility to measure the composition of layers on depth and of thin layers with thickness about sever nanometers by electron probe microanalysis. Simultaneous using of local cathodeluminescence allows characterization of point defects, charge carriers transport properties and their diffusion length. The rate of emission associated with quantum dots or quantum well layers with high charge carriers transport properties induces intensive luminescence related with this layer but weakly dependet on the electron beam energy. We use this method for the study of the laser heterostructures (ZnMgSSe-CdSe), a structure for HEMT transistors based on GaAs-AlxGa(1-x)As-InxGa(1-x)As and diode structures based on AlInGaN.

12:15 PM

Effects of Crystalline Strain and Defects in Electro-Optic Field Sensors: *Anthony Garzarella*[1]; Dong Ho Wu[1]; Syed Qadri[1]; [1]Naval Research Laboratory

Electro-optic (EO) sensors, used for the nonperturbative detection of electric fields, are strongly influenced by defects and strain in the nonlinear crystal. These effects can alter optical coherence of the probe beam, the nonlinear coefficient, and the effective value of the dielectric constant. In some cases, the optical modulation produced by the EO sensor is severely reduced, while in other cases, it can be enhanced by two orders of magnitude. In this report, we discuss these parasitic effects in detail, and how the can be exploited or suppressed to enhance the sensor responsivity.

12:30 PM Closing Remarks

Grid

	Glessner Auditorium	Banquet Rooms 1 - 3	Conference Registration Area
Sunday		Welcome Reception 7:30-9:00 p.m.	Meeting Registration 4:00-9:00 p.m.
Monday AM	Quantum Confined Strutures 8:30 a.m.-10:05 a.m. Morning Coffee Break 10:05-10:30 a.m. Electron Beam Imaging 10:30 a.m.-12:30 p.m.		Meeting Registration 7:30 a.m.-4:00 p.m
Monday PM	Industrial Instrumentation 1:30-3:30 p.m. Afternoon Coffee Break 3:30 p.m.-4:00p.m.	Lunch 12:30-1:30 p.m. Poster Viewing/Reception 4:30-7:00 p.m.	
Tuesday AM	Compound Photovoltaics 8:30-10:00 a.m. Morning Coffee Break 10:00-10:30 a.m. Defects in Silicon 10:30 a.m.-12:30 p.m.	Lunch 12:30-1:30 p.m.	Meeting Registration 8:00 a.m.-1:00 p.m.
Tuesday PM		Banquet Reception 6:00-6:45 p.m. Conference Banquet 6:45-8:30 p.m.	
Wednesday AM	Organic Photovoltaics and OLEDs 8:30-10:00 a.m. Morning Coffee Break 10:00-10:30 a.m. Defects in SiC 10:30 a.m.-12:30 p.m.		Meeting Registration 8:00 a.m.-4:00 p.m.
Wednesday PM	Defects in Nitrides 1:30-3:30 p.m. Afternoon Coffee Break 3:30-4:00 p.m. Defects in Devices 4:00-6:00 p.m.	Lunch 12:30-1:30 p.m.	
Thursday	X-Ray Topography 8:30 a.m.-10:00 a.m. Morning Coffee Break 10:00-10:30 a.m. Defects in Materials 10:30 a.m.-12:30 p.m. Closing Remarks 12:30-12:45 p.m.		Meeting Registration 8:00 a.m.-12:00 p.m.